JOURNAL OF GEOPHYSICAL RESEARCH, VOL. 106, NO. C8, PAGES 16,729–16,745, AUGUST 15, 2001

# Direct covariance air-sea $CO_2$ fluxes

W. R. McGillis and J. B. Edson
Woods Hole Oceanographic Institution, Woods Hole, Massachusetts

J. E. Hare
Cooperative Institute for Research in Environmental Sciences, University of Colorado
NOAA Environmental Technology Laboratory, Boulder, Colorado

C. W. Fairall
NOAA Environmental Technology Laboratory, Boulder, Colorado

**Abstract.** Direct covariance air-sea $CO_2$ flux measurements over the open ocean are reported. These measurements were performed during June 1998 in the North Atlantic within a significant $CO_2$ sink. These direct estimates are in general agreement with the traditional geochemical isotope constraints. The covariance, or eddy correlation, technique directly measures the air-sea $CO_2$ flux over hour timescales by correlating the fluctuations of $CO_2$ with the turbulent vertical velocity fluctuations in the atmospheric surface layer. These measurements quantify the transfer of $CO_2$ between the atmosphere and ocean over a range of wind speeds and improve the understanding of the environmental factors controlling the flux. The relatively large flux of $CO_2$ in the study region, together with improved analytical techniques, facilitated the measurements. The half-hour mean wind speeds varied from 0.9 to 16.3 m $s^{-1}$ over the month-long experiment. The mean $pCO_2$ during the study period was -85.8 ± 16.0 µatm, and the mean covariance $CO_2$ flux was estimated at 4.6 mol $m^{-2}$ $yr^{-1}$. The average observed wind speed was 7.7 m $s^{-1}$. This is in close agreement with 3.9 mol $m^{-2}$ $yr^{-1}$, the approximate $CO_2$ flux based on $^{14}C$ parameterizations at this wind speed. At high winds, where the relationship between gas physical properties, surface processes, and air-sea gas exchange is still elusive, direct $CO_2$ flux measurements are crucial. The measurements for winds in excess of 11 m $s^{-1}$ show a general enhancement of gas transfer velocity over previous indirect measurements, and it is believed that this enhancement can be explained by the fact that the indirect methods cannot discriminate surface process variability such as atmospheric stability, upper ocean mixing, wave age, wave breaking, or surface films.

## 1. Introduction

The ocean is a sink of a significant fraction of anthropogenically produced $CO_2$. Therefore understanding gas exchange across the air-sea interface is an important component in global climate dynamics. However, the kinetics of air-sea $CO_2$ transfer are difficult to study, as the many different mechanisms and processes that control the flux have large spatial and temporal variability. For example, the transfer or flux of $CO_2$ between the atmosphere and ocean $F_{CO_2}$ is commonly parameterized as

$$F_{CO_2} = k_{CO_2} \Delta CO_2 , \qquad (1)$$

where $k_{CO_2}$ represents the transfer velocity of $CO_2$ and $\Delta CO_2$ is the difference between the concentration of $CO_2$ in the bulk seawater and at the ocean surface. A more detailed description of (1) can be found in section 4.4.1, but here it should be noted that this expression encompasses the myriad processes controlling air-sea gas exchange; for example, the surface $CO_2$ can vary with temperature, salinity, bubble entrainment, and bioproductivity. In addition, the gas transfer rates are known to vary with wind speed, atmospheric stability, sea state, and a host of surface processes [*Jähne and Monahan*, 1995].

The quantification of $CO_2$ flux between the ocean and atmosphere is a controversial subject [*Broecker et al.*, 1986]. For example, indirect methods such as radiocarbon and radon provide transfer velocities ranging from 12 to 24 cm $h^{-1}$ [*Broecker and Peng*, 1982; *Jähne*, 1985; *Peng et al.*, 1979]. Most previous estimates of the transfer velocity using direct covariance flux estimates are at least an order of magnitude larger [*Jones and Smith*, 1977; *Wesely et al.*, 1982; *Smith and Jones*, 1985]. While these authors have provided a number of possible explanations for the observed differences, the actual cause of the discrepancies is ambiguous. One of the factors that remains to be adequately quantified is how certain environmental parameters influence the transfer velocity of $CO_2$, which, in turn, affects the flux. Many wind-wave experiments have shown that the gas transfer velocity is a function of wind speed [*Broecker et al.*, 1978, *Jähne et al.*, 1987]. However, the lack of sufficiently decisive data from field experiments has made relationships between wind speed and transfer velocity questionable when applied to the ocean. This is particularly true at high wind speeds, which are rarely sustained long enough to match the measurement time required by the indirect methods. Therefore large uncertainties in the estimation of air-sea $CO_2$ flux at moderate



Paper number 2000JC000506.
0148-0227/01/2000JC000506$09.00

to high wind speeds exist, particularly where the gas transfer is nonlinearly related to the wind speed [*Wanninkhof*, 1992; *Wanninkhof and McGillis*, 1999].

As a result of the uncertainty, climate models employ differing transfer velocity parameterizations, which ultimately produce a wide variety of long-term climate forecasts. The use of a single accurate parameterization for the $CO_2$ transfer velocity in all climate models would remove one major source of ambiguity. Therefore direct measurements of the $CO_2$ flux over a wide range of wind speeds are required to improve these transfer velocity parameterizations. In particular, the direct covariance technique has the potential to circumvent many of the problems associated with indirect measurements of gas exchange because it is a measurement of the gas flux at the scale of the turbulent transport. Following are reported results from the use of the covariance technique to obtain direct air-sea $CO_2$ flux measurements during a field experiment performed in the North Atlantic.

## 2. Interdisciplinary Air-Sea Gas Exchange Experiment: GasEx-98

In May and June of 1998 an interdisciplinary air-sea gas exchange experiment, named GasEx-98, was performed in the North Atlantic at 46°6'N and 20°55'W aboard the National Oceanic and Atmospheric Administration (NOAA) R/V *Ronald H. Brown*. This cruise included a wide range of independent air-sea gas exchange measurement efforts, which were simultaneously conducted for comparison. Specifically, estimates of air-sea gas exchange are derived from deliberate-release dual-tracers ($SF_6$ and the isotope $^3He$), dimethylsulfide atmospheric gradients, $CO_2$ atmospheric gradients, and direct covariance $CO_2$ measurements. The deliberate tracer release also served as a water mass marker, as the overall experiment was conducted within a persistent warm-core eddy with a cool top. Drifting marker buoys were deployed during the experiment to follow the movement of the eddy. Tagging water parcels with deliberate tracers and drifters is useful to perform a successful Lagrangian process study, as the tracers can clearly delineate a homogeneous water parcel. At later stages when the tracer patch becomes more chemically heterogeneous, natural tracers such as salinity and $CO_2$ are necessary. The interdisciplinary investigations performed during this study indicate a cruise yielding several important breakthroughs in the understanding of air-sea $CO_2$ fluxes and biogeochemical cycles.

## 3. Approach

The well-established direct covariance or eddy correlation measurement technique is the standard for surface layer gas flux measurements as it is a direct computation of the covariance of the gas concentration with the air vertical velocity at the height of measurement. This method assumes that the mixing ratio of scalar species $c$ can be decomposed into mean and fluctuating components

$$r_c = \overline{r_c} + r_c', \tag{2}$$

where $r_c$ is the mixing ratio for the gas and is defined as the mass of $c$ per unit mass of dry air, the overbar denotes an average of the gas concentration over a large ensemble of turbulent eddies, and the prime denotes the fluctuations from this average. By definition, the kinematic vertical flux of a scalar species $F_c$ is

$$F_c = \rho_a \overline{w' r_c'}, \tag{3}$$

where $w'$ represents the turbulent fluctuations in the vertical component of the wind and $\rho_a$ is the density of dry air, which is assumed to have a constant value in the following discussion. Estimates of ensemble averages are made to within some statistical sampling uncertainty with the appropriate selection of an averaging time interval [*Mahrt et al.*, 1996].

This expression demonstrates the potential ease with which eddy correlation estimates of the turbulent fluxes can be made with sonic anemometers and fast response gas analyzers. It appears that all that is necessary to obtain the turbulent flux is the computation of the covariance. However, on a seagoing research vessel the measurement of the velocity components necessary to compute the covariance becomes difficult because of the platform motion. In the case of a ship the anemometer is fixed and moves with it, requiring significant correction to the measured vertical wind velocity component. The superstructure of the ship also causes flow distortion and additional uncertainty in the flux estimates. In the specific case for $CO_2$ where commercial sensors with sufficient rapid response are available, attention must be paid in signal processing. This is due to the generally low signal-to-noise ratio (SNR) found in oceanic conditions because of the small air-sea concentration difference.

Therefore concerns related to the application of the direct covariance method at sea include (1) the ability to adequately remove the motion contamination, (2) deployment of the sensor package at a location that minimizes the effect of flow distortion around an oceangoing vessel, and (3) having adequate signal levels and frequency response to compute the gas flux using currently available sensors. In sections 3.1- 3.3 these concerns are addressed, and the flux system and analysis scheme for computing the fluxes are outlined.

### 3.1. Direct Covariance Flux System

To accomplish the objective of obtaining direct $CO_2$ flux measurements from a ship, a turbulent flux measurement system was placed on the forward jack staff of the Brown. As on any seagoing research vessel, the measurement of the vertical wind velocity necessary to compute the covariance is complicated by the platform motion, and this motion contamination must be removed before the fluxes can be estimated. The error arises from three sources: instantaneous tilt of the anemometer due to the pitch, roll, and heading variations of the ship; angular velocities at the anemometer due to rotation of the ship about its local coordinate system axes; and translational velocities of the ship with respect to a fixed frame of reference.

The integrated Direct Covariance Flux System (DCFS) is capable of correcting for the velocity of the ship motion [*Edson et al.*, 1998]. The heart of the DCFS is the Solent three-axis ultrasonic anemometer-thermometer and a Systron-Donner MotionPak system of three orthogonal angular rate sensors and accelerometers. The MotionPak is mounted directly beneath the sonic anemometer, which allows accurate alignment with the sonic axes in addition to ensuring that the wind and motion measurements are collocated. The

application of this "strap-down" system allows us to express the true wind vector as

$$\mathbf{V}_{true} = \mathbf{T}\,(\mathbf{V}_{obs} + \mathbf{\Omega}_{obs} \bullet \mathbf{R}) + \mathbf{V}_{mot}\,. \quad (4)$$

$\mathbf{V}_{true}$ is the desired wind velocity vector in the Earth reference coordinate system; $\mathbf{V}_{obs}$ and $\mathbf{\Omega}_{obs}$ are the measured wind and platform angular velocity vectors in the ship frame of reference, respectively; $\mathbf{T}$ is the coordinate transformation matrix from the ship frame coordinate system to the reference coordinates; $\mathbf{R}$ is the position vector of the wind sensor with respect to the motion package and is negligible for the strap-down configuration; and $\mathbf{V}_{mot}$ is the translational velocity vector measured at the location of the motion package.

A more complete description of the DCFS, including an analysis of the ship-induced flow distortion, is given by *Edson et al.* [1998]. On the *Brown*, the DCFS system was deployed on the forward jack staff directly above the bow. This placed the anemometer 18 m above the mean sea surface. Relative wind directions used in the analysis where limited to $\pm 60°$ of the bow. The tilt in the airflow measured by the sonic anemometer (i.e., the tilt remaining after motion correction) varied less than 4° for these wind directions.

The corrected velocity components from these relative wind directions are used to compute the covariance momentum, gas, sensible heat, and water vapor fluxes. For example, the momentum flux is described by

$$\tau = \rho \overline{u'w'}\,, \quad (5)$$

where $\rho$ is the density of moist air and $u$ and $w$ are the longitudinal and vertical wind velocity components, respectively. Friction velocities were directly measured with eddy correlation as

$$u_* = (-\overline{u'w'})^{1/2}\,. \quad (6)$$

The friction velocities from GasEx-98 are shown in Figure 1. The friction velocities estimated from the bulk flux algorithm are described by *Fairall et al.* [1996]. The variability in the measurements is consistent with current direct flux measurements.

### 3.2. Measurement of Mean $pCO_2$ Concentrations

The air and water $CO_2$ measurements were obtained with two independent closed-path nondispersive infrared (NDIR) Licor-6262 detector instruments. Closed-path (and most open-path) $CO_2/H_2O$ NDIR instruments are based on the molecular absorption of infrared radiation for the species of interest. For $CO_2$ the common choice of absorption band is at 4.26 μm. This wavelength exhibits relatively strong absorption, and fairly simple sources and detectors are readily

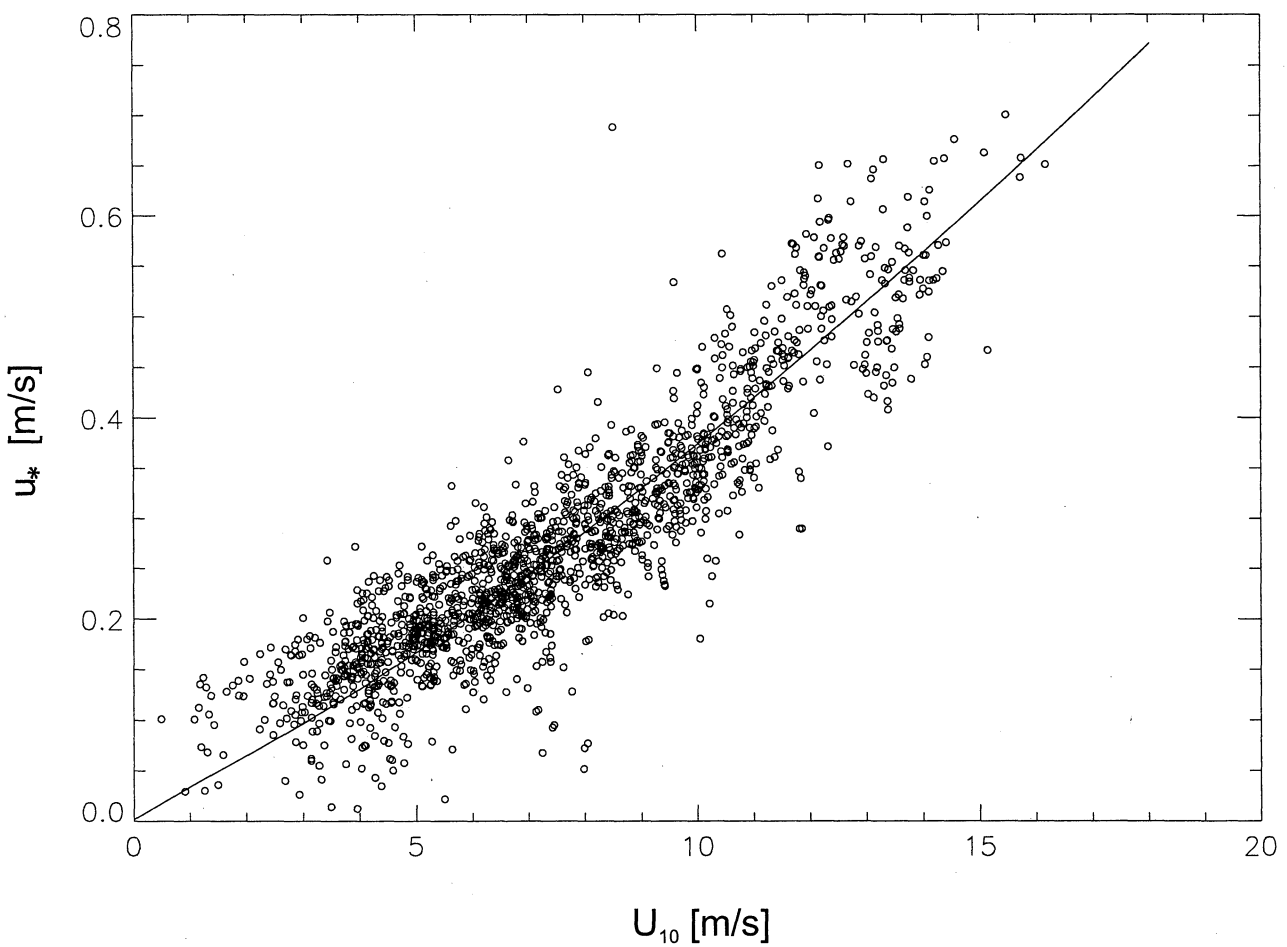


**Figure 1.** Friction velocity versus 10-m wind speed corrected to neutral conditions. The solid line is the bulk model prediction.

available. Similarly, a strong $H_2O$ absorption band lies at 2.59 μm, and an additional band with very low absorption is used as a reference. This reference is used to discern changes in absorption which are not related to the concentration of the gas, such as that due to dirt on the optics or variations in emitted radiation. The absorption of infrared radiation through the measurement path is proportional to the ratio of the returned signal in the absorption band to that of the reference.

The water-side $CO_2$ mean concentration measurements were obtained from the headspace gas of an equilibrator with one of the NDIR detectors. Equilibration of the sample gas with ocean water was done by continuously pumping and draining seawater into an enclosed chamber. Gas was pumped from the headspace of the chamber, through a condenser that removes approximately 90% of the $H_2O$, and through a $Mg(Cl0_4)_2$ drier. The gas then passed through the detector and back to the equilibrator. The output from the detector was corrected for the effects of pressure, temperature, and any remaining $H_2O$ on the measured $CO_2$ concentration. Additionally, as with most fast response $CO_2$ sensors, the Licor-6262 used in this manner measures the $CO_2$ partial pressure, $pCO_2$. The two measurements are related using

$$CO_{2_w} = s\, pCO_{2_w}, \tag{7}$$

where $s$ is the solubility of $CO_2$, which is a function of temperature and salinity.

Mean air-side $pCO_2$ estimates were also obtained with a similar NDIR. The analyzer was deployed on a scaffold erected 5 m behind the forward jack staff and 6 m below the sonic anemometer. The intake for the NDIR was placed directly behind the sonic sampling volume by attaching the sampling tube to one of the supporting struts. The total length of the tube from the sonic anemometer to the analyzer was approximately 13 m. Flow controllers precisely regulated the flow rate of 10 L $min^{-1}$, resulting in a calculated time lag of approximately 1 s (the inside diameter of the tube was 0.4 cm). Measurements of the lag by injecting $CO_2$ into the intake and recording the time of detection showed the actual lag to be 1.2 s.

The use of (1) requires measurement of the mean $CO_2$ concentration at the surface, which is extremely difficult to measure in the field. However, since $CO_2$ is primarily liquid phase controlled because of its low solubility [*Liss and Slater,* 1974; *Businger*, 1997; *McGillis*, 2000], a very small gradient exists on the air side of the interface. This allows the surface concentration to be closely approximated by the measured air-side concentration, such that $\Delta CO_2$ is often approximated using the air-sea concentration or partial pressure differences

$$\Delta CO_2 = CO_{2_w} - \frac{CO_{2_a}}{H} = s\Delta p CO_2, \tag{8}$$

where $H$ is Henry's law parameter. The partial pressure approach is used with the current system. Note that while the small gradient is advantageous in this instance, it is the primary cause for the difficulties associated with making direct $CO_2$ flux measurements over the ocean. The approach used to overcome these difficulties is given in section 3.3.

### 3.3. Direct Covariance $CO_2$ Flux Measurements

Generally, over-ocean $CO_2$ fluctuations are relatively small because of the small air-sea concentration differences. During GasEx-98, substantial increases in $CO_2$ flux were found by conducting the experiment in a $CO_2$ sink region with a much larger than average concentration difference and moderate to high winds. However, even with these advantageous environmental conditions, any means to improve the flux system SNR is always desirable. Therefore applying all appropriate corrections to the measurements and optimization of the setup to reduce system noise is crucial to obtain accurate flux estimates.

The signal strength is a function of the air-sea concentration difference and the wind speed. The noise in the system is due to a number of factors such as pressure fluctuations resulting from pump noise and unavoidable limitations of NDIR analyzers used in the systems such as $H_2O$ dilution effects and optical cross talk. Noise in the $CO_2$ flux system is reduced by (1) regular automated calibration of the system using 0.005-ppm accurate gas standards, (2) reduction of the vacuum pump pressure noise fluctuations with a flow reservoir, (3) incorporating an in-line heat exchanger to minimize temperature fluctuations, (4) implementing flow controllers to ensure constant intake-to-sample lags, and (5) performing simultaneous data acquisition of all relevant meteorological flux parameters. Additional corrections and sources of noise are described in sections 3.3.1 - 3.3.4.

**3.3.1. Dilution effects.** If the gas sensor measures the mixing ratio $r_c$, then the flux of that trace gas is simply the correlation with vertical velocity as expressed in (3). However, it is more common for gas analyzers to provide a measurement of mass concentration, and *Webb et al.* [1980] showed that the flux must be corrected for the density variations caused by $H_2O$ and temperature. Under conditions of constant total pressure and trace gas mixing ratio the correction is expressed as

$$\rho_a r_c' = c' + c\left[\frac{m_a \rho_v'}{m_v \rho_a} + \left(1 + \frac{m_a \rho_v}{m_v \rho_a}\right)\frac{T'}{\overline{T}}\right], \tag{9}$$

where $m_a$ and $m_v$ are the molecular weights of dry air and water vapor, respectively, $\rho_v$ is the mean water vapor density, and $T$ is the temperature. The result of this dilution effect is that in the absence of fluctuations in the mixing ratio of the trace gas the temperature and humidity perturbations will cause variations in $c$. The dilution effect corrections are necessary in all forms of micrometeorological mass concentration measurement methods (direct covariance, spectral, or gradient methods). For direct covariance flux measurements the correction is

$$F_c = \overline{w'c'} + c\left[\frac{m_a}{m_v \rho_a}\overline{w'\rho_v'} + \left(1 + \frac{m_a \rho_v}{m_v \rho_a}\right)\frac{\overline{w'T'}}{\overline{T}}\right] = \overline{w'c'} + \overline{w}c, \tag{10}$$

where the small mean vertical velocity $\overline{w}$ can be interpreted as that required to maintain the density of dry air in the presence of sensible and latent heat fluxes. As expressed by *Fairall et al.* [2000], for $CO_2$ the two terms in (10) are often of similar magnitude and opposite sign. It is therefore necessary to very accurately estimate the sensible heat and water vapor fluxes, particularly if an open-path system is used where the user has no control over temperature and humidity fluctuations.

**3.3.2. Optical cross-sensitivity.** In addition to the dilution effect, optical cross-sensitivity due to the presence of

water vapor must be considered [*Kohsiek*, 2000]. The presence of water vapor causes a broadening of the absorption bands with the gas analyzer. This can result in some overlap or optical cross talk between the infrared absorption bands of the $CO_2$ and $H_2O$ channels. The cross-sensitivity is defined as the apparent change in $CO_2$ density when the water vapor is increased in a constant pressure and temperature environment. The resulting cross-sensitivity correction is particularly important where the flux of $CO_2$ is small and the flux of water vapor is large, which are the prevalent conditions over the ocean.

The cross-sensitivity is typically expressed as a dimensionless coefficient $\beta$, which is the apparent change in $CO_2$ mass concentration induced by a change in water vapor mass concentration. The dilution effect as expressed in (9) is a form of cross-sensitivity, and the water vapor contribution to $\beta$ is estimated to be about $-10^{-3}$ [*Fairall et al.*, 2000]. According to *Kohsiek* [2000] there are five recognized sources of cross talk within this type of gas analyzer: (1) Light is absorbed in the $CO_2$ or reference channel by $H_2O$. This is a very small effect ($\beta \sim 10^{-5}$) and can be ignored. (2) Absorption of light at wavelengths outside the passband of the $CO_2$ channel is not completely suppressed by the filter. This effect is ~2 orders of magnitude less than the dilution effect ($\beta \sim 10^{-5}$) and therefore can be neglected. (3) Water molecules can form pairs, called dimers, under high relative humidity conditions, but this is presently assumed negligible. (4) Pressure broadening is caused by collisions of $CO_2$ molecules with the other atmospheric constituents: nitrogen, oxygen, water vapor, etc. These collisions broaden the absorption lines, and the degree of broadening depends on the local pressure. The Licor-6262 manufacturer gives a value $\beta = 1.4 \times 10^{-4}$ for the combined effects of optical cross talk.

Clearly, infrared absorption by $CO_2$ is sensitive to pressure, humidity, and temperature because of both the cross-sensitivity and the dilution effect (note that an additional pressure term in (9) and (10) was neglected by assuming constant pressure). These effects show why drying and thermally equilibrating the incoming air sample can minimize the corrections for a closed-path configuration, which was the approach taken by the NOAA Climate Monitoring and Diagnostics Laboratory group during GasEx-98. The flux system deployed during GasEx-98 was designed to minimize the temperature and pressure fluctuations using in-line thermal and pressure equilibration and correct for the water vapor effects using (10) for dilution and the Licor correction for pressure broadening. The atmospheric $CO_2$ fluctuations were measured by pulling air samples through the closed-cell NDIR described in section 3.2, which simultaneously measured water vapor concentration in the air sample. In-line thermal and pressure equilibration was achieved in the sampling system using a .003-$m^3$ pressure reservoir and a 1.5-m-long, 6.4-mm diameter copper tube heat exchanger.

**3.3.3. Sampling tube effects.** Because a closed-path gas analyzer requires the use of tubing to bring the sample air into the measurement cell, some limitations and potential sources of error are also imposed. The tube acts as a low-pass filter and attenuates the small-scale fluctuations of the gas concentration, which may cause an underestimation of the flux. Corrections are available according to theory as outlined by *Leuning and Moncrieff* [1990], *Suyker and Verma* [1993], and *Leuning and Judd* [1996]. These corrections are required when the half-power frequency of the low-pass filter is less than the highest frequency responsible for turbulent transport [*Leuning and Judd*, 1996]. The half-power frequency is typically formulated in terms of the Reynolds number for the flow in the tube defined as

$$Re = \frac{d_t U_t}{\nu_a}, \tag{11}$$

where $d_t$ is the inside tube diameter, $U_t$ is the flow velocity in the tube, and $\nu_a$ is the kinematic viscosity of air. The flow rate and tube diameter used in GasEx-98 give a Reynolds number of 3550, which is representative of turbulent pipe flow.

Using the expressions given by *Leuning and Judd* [1996], the system used to sample the air during the investigations should have a dimensionless cutoff filter between 0.04 and 0.1 based on the results of *Massman* [1991] and *Lenschow and Raupach* [1991]. According to *Kaimal et al.* [1972], 95% of the scalar flux occurs below a cutoff frequency described in terms of wind speed and height above the surface $f_c = 2U/z$ for neutral to unstable conditions. *Leuning and Judd* [1996] used this cutoff frequency to derive an expression for the dimensionless cutoff frequency in terms of the tube flow parameters

$$n_c = \frac{4 r_t^{3/2} L_t^{1/2} U}{\nu_a z Re} \tag{12}$$

where $r_t$ is the tube radius and $L_t$ is the tube length. These expressions imply that the system captured most of the turbulent flux as long as $n_c < 0.04$ (using the more conservative estimate given by *Massman* [1991]). The sensor package on the *Brown* was located 18 m above the sea surface. Therefore this system measures all turbulent fluctuations that contribute to the flux for wind speeds less than 30 m $s^{-1}$.

In addition to the dampening of small-scale signals there is evidence that long-term use of tubes (over the course of weeks) will result in dirt and possible salt contamination on the walls of the tubing [*Leuning and Judd,* 1996]. Although in-line particle filters are used in the setup to prevent corruption of the gas analyzer cell, it is unclear at this time what deleterious interactions may occur between the contamination and water vapor in the line. *Leuning and Judd* [1996] report a decrease in response for water vapor after several weeks but little deterioration of the $CO_2$ signal over this same period. Therefore, during GasEx-98, attempts to minimize the damping of the signals and contamination in the tube were made through the use of the shortest possible tube between the sonic anemometer and NDIR. Water vapor measurements from the NDIR are only used to correct for dilution and pressure broadening (the vapor flux is measured using the open-path NDIR).

**3.3.4. Gyroscopic effects.** An additional source of noise was discovered during GasEx-98. This was a result of gyroscopic effects on the chopper wheel in the NDIR detector caused by wave-induced motion. As a result, the speed of the chopper wheel was affected by platform accelerations causing additional noise in the system. Both the $CO_2$ and $H_2O$ channels detect this error, but the water vapor flux is not significantly altered because that signal is much larger than this noise source.

Constant calibration of the closed-path NDIR was performed throughout the duration of the cruise by flushing

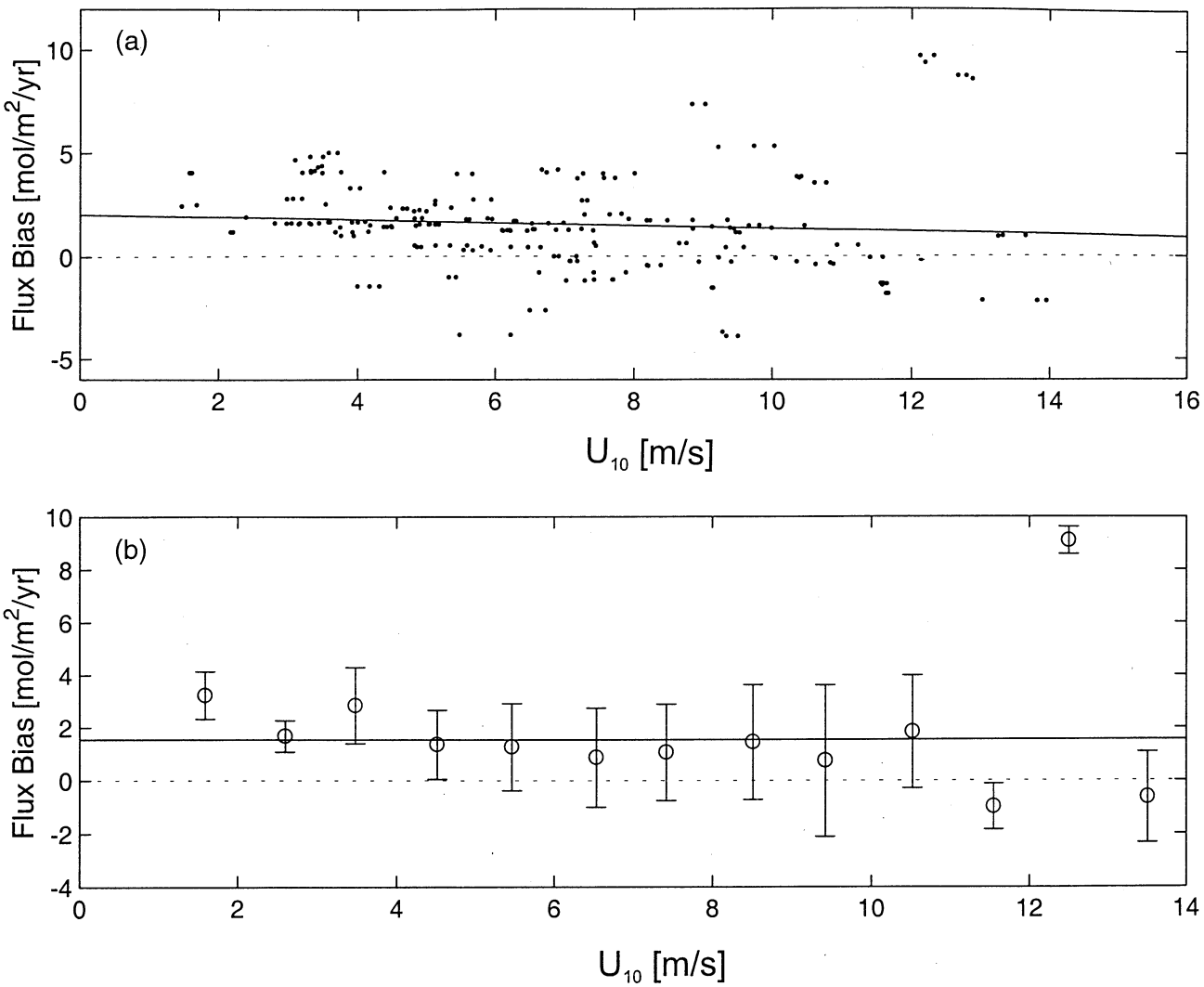


**Figure 2.** Covariance estimates of flux bias computed during calibration periods. Nonzero estimates of the flux are primarily caused by wave-induced accelerations of the NDIR chopper wheel. (a) Linear fit to all data given by -0.07 $U_{10}$ + 2.03 mol $m^{-2} yr^{-1}$ (b) bin-averaged values and a constant fit to 1.6 mol $m^{-2} yr^{-1}$.

$CO_2$-free gas through the analyzer for 10 min every 4 hours. This provides a regular operational measure of the random and ship-induced noise. More importantly, it provides a means to quantify the systematic error due to the combined noise sources in the flux estimates. Toward this end, the covariance of zero gas with the motion-corrected vertical velocity fluctuations was computed during every calibration period using 3 min of the calibration time series, insuring that the zero gas has equilibrated in the system and that the computed covariance includes many wave periods. Prior to the computation of the cospectrum, the detector signal was lagged by 1.2 s to mimic the procedure used to compute the $CO_2$ flux.

The systematic errors/biases (i.e., different from sampling variability) in the covariance estimates computed from the integrated cospectra are shown in Figure 2. A least squares fit to the data in Figure 2a shows a positive bias (y intercept of 2.03 mol $m^{-2} yr^{-1}$) that slowly decreases with increasing wind speed (slope of -0.07 mol $m^{-3} yr^{-1}$). If the wind speed dependence is neglected, the mean estimate from the null tests implies that the ship-induced noise can produce a flux of 1.6 ± 2.3 mol $m^{-2} yr^{-1}$. This bias is shown by the solid line in Figure 2b, which provides good agreement with the bin-averaged values between 2 and 11 m $s^{-1}$.

The analysis has also shown that the noise is substantially larger in the $CO_2$ variance estimates computed from the autospectra. However, the noise in the cospectral estimates has been reduced by two important factors: (1) the motion correction of the vertical velocity signal, which removes most of the ship-induced motion and greatly reduces the coherence with the ship-induced noise in the NDIR, and (2) the lag required to synchronize the $CO_2$ and vertical velocity signals. This further reduces the cospectra (while increasing the quadrature spectra) by introducing a phase lag to the motion-induced signal but not the desired correlation.

## 4. Results and Discussion

### 4.1. Environmental Conditions

Air-sea gas transfer is typically parameterized in terms of a transfer velocity and the gas concentration difference across the air-sea interface as shown in (1). The gas transfer velocity is commonly parameterized as a function of mean wind speed [e.g., *Liss and Merlivat*, 1986; *Wanninkhof*, 1992;

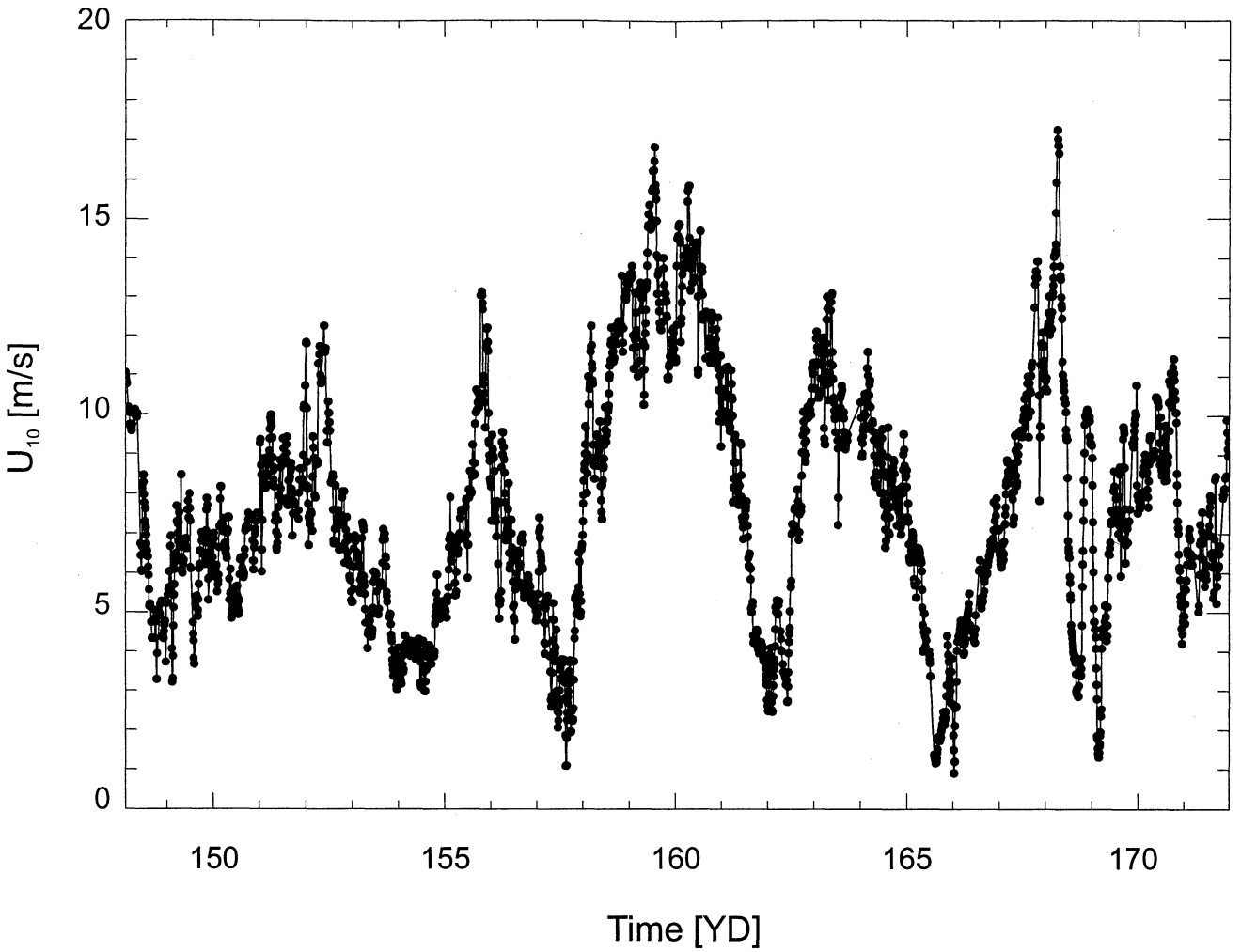


**Figure 3.** Time series of 10-m wind speed during GasEx-98 in the North Atlantic measured using an ultrasonic anemometer corrected for ship motion. The sonic anemometer was mounted on the forward *Brown* bow mast. Wind speeds varied on hourly scales and over a wide range with gusts up to 17 m $s^{-1}$. The study site location was approximately 46°6′N and 20°55′W in a warm-core eddy.

*Wanninkhof and McGillis*, 1999]. Therefore the gas flux is expected to vary with both wind speed and the air-sea $CO_2$ concentration difference. Continuous measurements of the 10-m mean wind speed are shown in Figure 3. These observations show that a number of atmospheric disturbances passed through the study area with wind speeds in excess of 8 m $s^{-1}$. The frequency of these meteorological systems was approximately every 4 days with sustained wind speeds greater than 10 m $s^{-1}$ persisting from a few hours to more than a day.

The GasEx-98 study site was chosen on the basis of the strength and constancy of the air-sea $pCO_2$ difference, as shown in Figure 4. The average $\Delta pCO_2$ during the course of the study period was -85.8 ± 16.0 μatm. This concentration difference is relatively large for ocean surface waters and greatly increased the ability to measure the flux. Observations of the individual concentrations showed a slowly varying $pCO_2$ concentration in the ocean. The shorter-term fluctuations are driven by variability of the mean atmospheric $pCO_2$ that resulted in $\Delta pCO_2$ levels between -70 and -110 μatm. The concentration difference varies substantially on timescales of less than a day, which demonstrates the necessity for direct measurements of the flux.

Initially, an algal bloom continued to increase the $\Delta pCO_2$ magnitude. The temporary decrease on year day (YD) 156 and the more permanent decrease on YD 158 were caused by high-wind events entraining water masses from below that input carbon and nutrients into the mixed layer. On the basis of these preliminary results it has been hypothesized that these episodic events, to a large extent, control the evolution of the spring blooms and $pCO_2$ in the area. After YD 166 the algal bloom decayed, and the warm-core eddy began to dissipate, and this fact is reflected in the reduced mean and increased variability of the $\Delta pCO_2$.

### 4.2. Direct Flux Estimates

Continuous covariance $CO_2$ fluxes were performed for 24 days during GasEx-98. The $CO_2$ concentration, water vapor concentration, pressure, and temperature were sampled in the closed cell at 20 Hz and averaged to 4 Hz. The raw time series were detrended and time-tapered with a Hamming window; estimates of $CO_2$ flux were computed by integrating

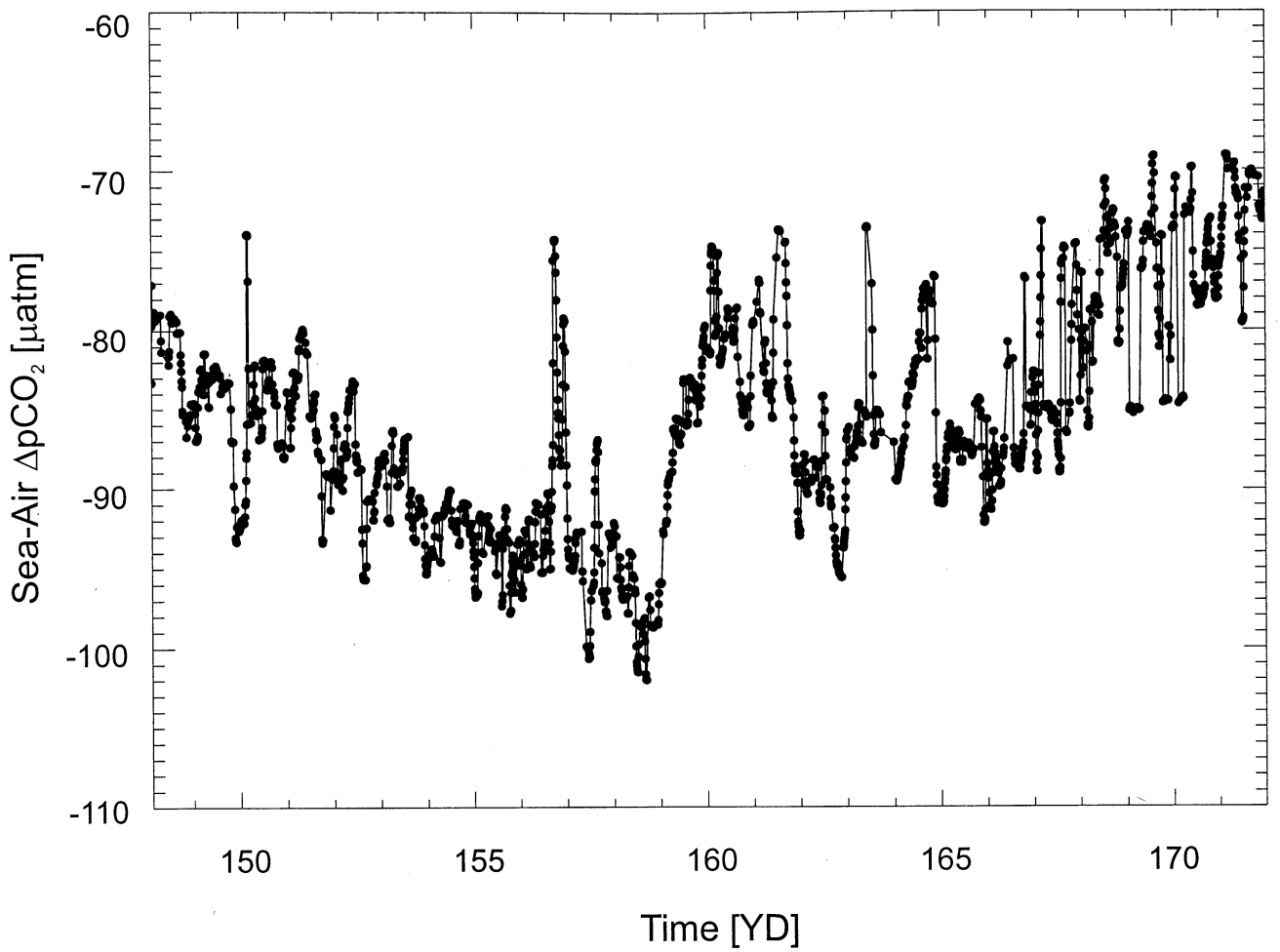


**Figure 4.** Time series of sea-air $pCO_2$ differences during GasEx-98.

the cospectrum. The wind fluctuations were correlated with the $CO_2$ mixing ratio using the measured 1.2-s lag. It should be noted that sensitivity tests were conducted by varying the lag between 1 and 1.5 s. These tests showed that the value of the fluxes changed by less than 5% over this range.

The directly measured *wc* cospectra, averaged in wind speed bins from the entire GasEx-98 deployment, are shown in Figure 5. The cospectral levels increase with increasing wind speed, but the overall shape of each cospectrum is similar. The figure also shows the average *wc* cospectrum computed during the calibration periods over a 1-day period. The cospectra show signs of this wave-induced signal and noise at the wave frequencies, which accounts for some of the uncertainty in the flux estimates as described in section 3.3.3.

The raw covariance $CO_2$ flux and the null flux measurements are plotted in Figure 6. The null flux is determined during calibration periods. The null flux magnitude shows a bias due to the motion cross talk from gyroscopic effects. At wind speeds below 4 m $s^{-1}$ the bias is comparable to the measured flux, which results in large uncertainties in the low-wind-speed estimates. However, above approximately 4 m $s^{-1}$ the measurements become comparable and then significantly larger as a wind speed of 16 m $s^{-1}$ is approached.

The combination of the various noise sources contributes to the uncertainty in the flux estimates. A useful way to quantify this is to treat the uncertainty due to $w'$ and $\rho_a r_c'$ separately. The analysis given by *Edson et al.* [1998] shows that the uncertainty in the flux estimates that arises from inadequate motion correction is approximately 15% in the momentum flux or 8% in $u_*$. The uncertainty in $u_*$ is a good approximation for the uncertainty in the ability to accurately measure $w'$. This estimate gives an uncertainty of 0.3 mol $m^{-2}$ $yr^{-1}$ when applied to the mean of the flux estimates shown in Figure 6.

The uncertainty due to $\rho_a r_c'$ is dominated by the dilution correction and the gyroscopic effect. The uncertainty in the dilution correction due to temperature fluctuations is negligible compared to the water vapor correction because of thermal equilibration. The upper limit of the uncertainty in the dilution correction can be approximated using the RMS difference between the $\overline{w'\rho_v'}$ correlations measured by the open- and closed-path NDIR sensors ($w'$ is the same in both cases). If the temperature flux term is neglected and the RMS difference is used in place of $\overline{w'\rho_v'}$ in (10), a value of 2.1 mol $m^{-2}$ $yr^{-1}$ is obtained.

The uncertainty in the dilution correction can be approximated by dividing by the mean flux estimates. Likewise, the uncertainty due to the wave-induced gyroscopic effects can be approximated by the standard deviation of the fluxes computed during the null test (i.e., 2.3 mol $m^{-2}$ $yr^{-1}$) divided by the mean flux estimates. The total uncertainty in

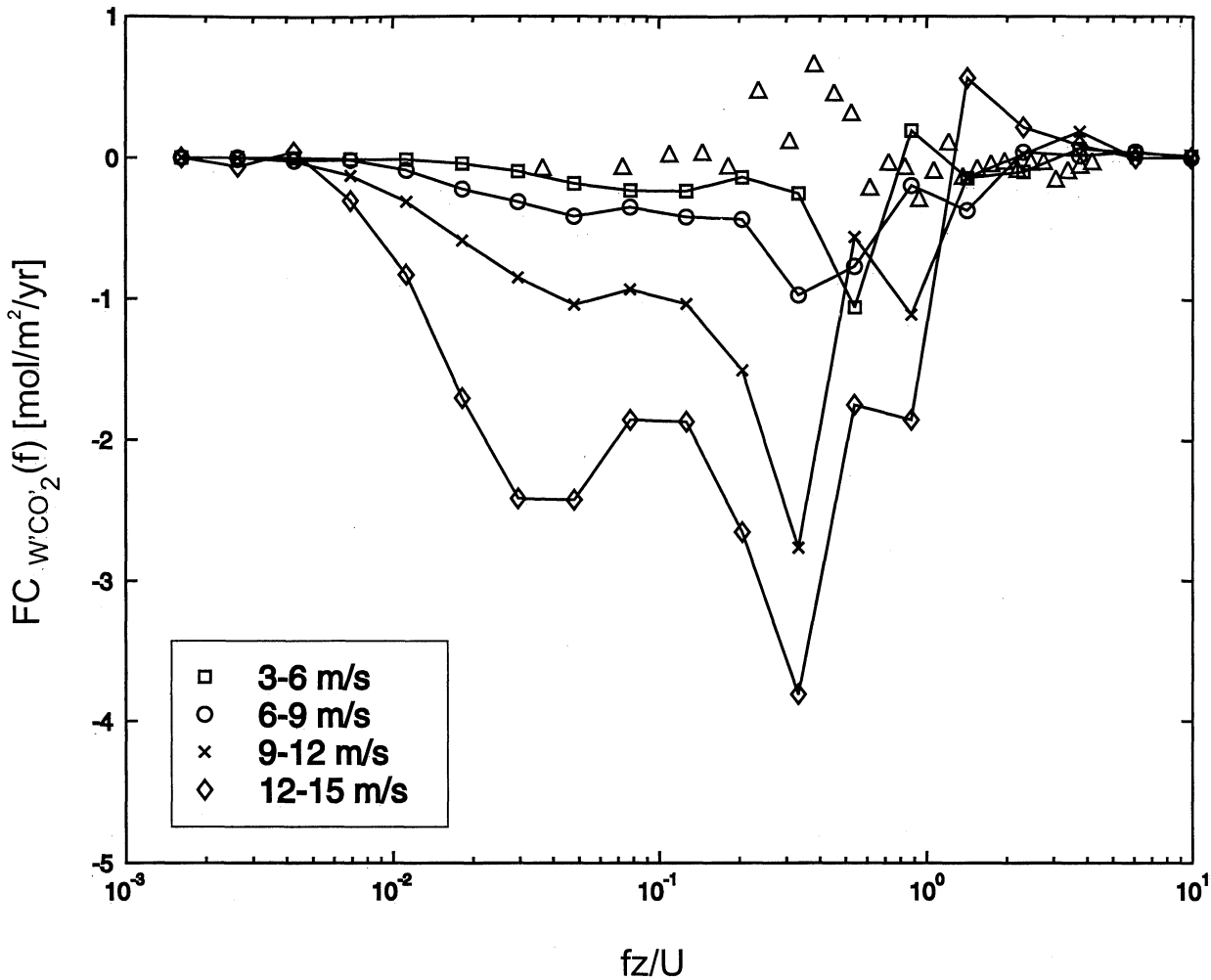


**Figure 5.** Cospectra of vertical wind fluctuations and atmospheric $CO_2$ fluctuations measured during GasEx-98 with the direct covariance $CO_2$ flux system. Ensemble spectral densities for the wind speed range 3-6 m s$^{-1}$ (squares), 6-9 m s$^{-1}$ (circles), 9-12 m s$^{-1}$ (crosses), and 12-15 m s$^{-1}$ (diamonds). Cospectra of vertical wind fluctuations and zero reference gas measured during calibration intervals (triangles) are shown for comparison. The NDIR chopper wheel is affected by rotational accelerations, and the predominant noise occurs at the frequency of ship motion caused by waves.

the individual flux estimates can be approximated by the sum of the squares of the uncertainties. The trend shown in Figure 6 indicates that the total uncertainty is expected to decrease with increasing wind speed due to the overall increase of the measured flux. Using the median values from this figure, the uncertainty in the individual flux estimates ranges from greater than 100% at wind speeds less than 7 m s$^{-1}$ to 70% at 9 m s$^{-1}$ to less than 30% above 12 m s$^{-1}$.

A time series of the 30-min cospectral estimates of the $CO_2$ flux after removal of the bias due to motion cross talk is shown in Figure 7. During the periods of high winds, $CO_2$ fluxes into the ocean often exceeded 15 mol m$^{-2}$ yr$^{-1}$, and the variability of the flux occurs on timescales of less than a day. This is consistent with the results shown in Figures 3 and 4, which display the same variability in two of the fundamental parameters governing $CO_2$ gas exchange, i.e., wind speed and air-sea concentration difference.

### 4.3. Uncertainty Analysis

A more rigorous uncertainty analysis can be conducted using these results and the approach suggested by *Fairall et al.* [2000]. This approach begins by defining the mass concentration used in (10) as

$$c = \rho_a \frac{e_c m_c}{m_a P_a}, \tag{13}$$

where $m_c$ is the molecular weight of $CO_2$ and $e_c$ and $P_a$ are the partial pressures of $CO_2$ and dry air, respectively. The $CO_2$ flux can then be expressed by rewriting (10) as

$$F_c = \overline{w'c'} - (\beta_{dv} + \beta)\overline{w'\rho_v'} - \rho_a\left(1 + \frac{m_a \rho_v}{m_v \rho_a}\right)\beta_{dT}\frac{\overline{w'T'}}{\overline{T}}, \tag{14}$$

where the $\beta$ coefficients express the various forms of cross talk that influence the measurement of the flux: $\beta_{dv} = -m_c e_c / m_v P_a = 8.8 \times 10^{-4}$ is the $CO_2$ dilution effect for water vapor, $\beta_{dT} = -m_c e_c / m_a P_a = 5.5 \times 10^{-4}$ is the dilution effect for temperature, and $\beta = 1.4 \times 10^{-4}$ is the water vapor cross talk coefficient for the Licor-6262.

The uncertainty in the flux $\delta F_c$ can be estimated using the standard derivative expansion

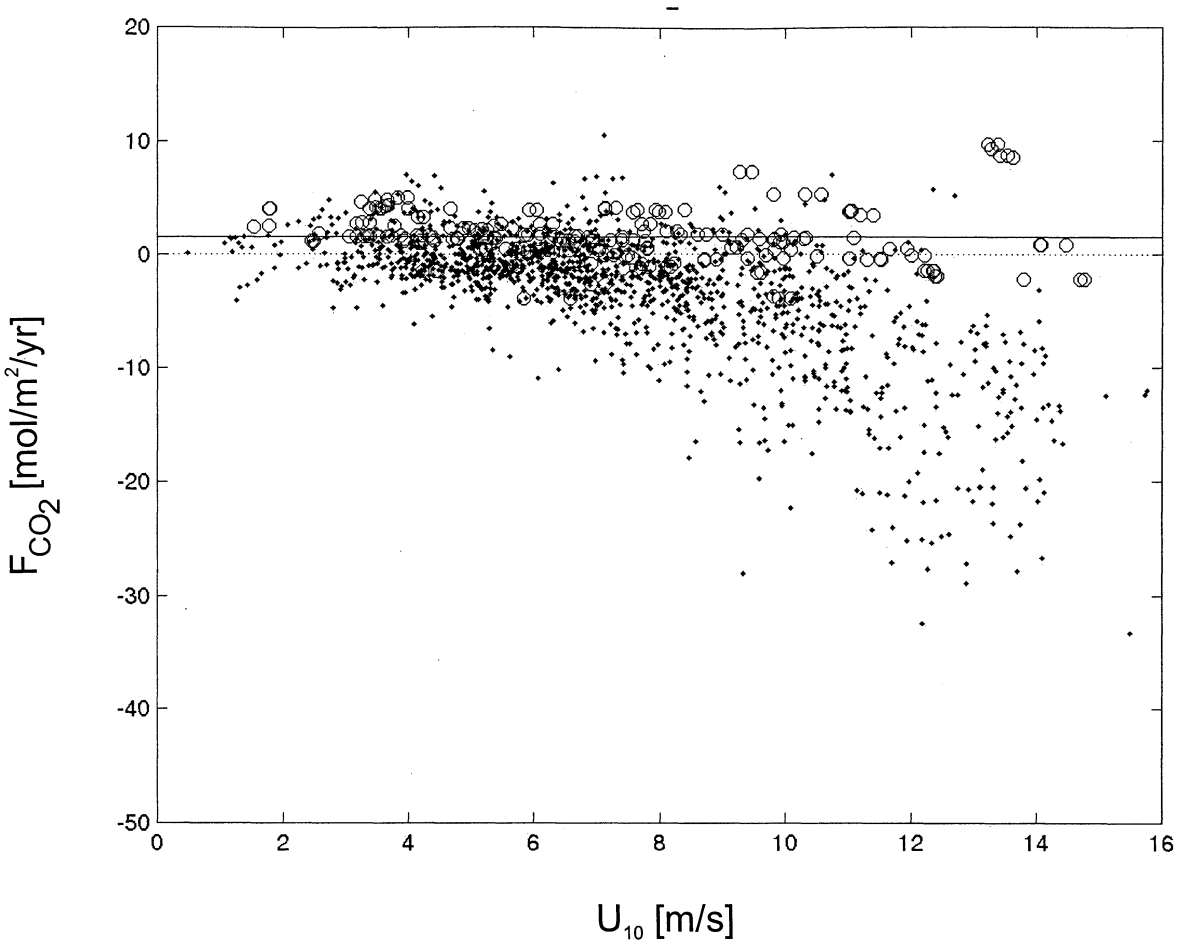


**Figure 6.** Direct covariance $CO_2$ flux estimates performed during GasEx-98 (solid points). Flux biases determined from null tests are shown for comparison (open circles).

$$\delta F_c = -(\beta_{dv} + \beta)\delta\overline{w'\rho_v'} - \delta\beta\overline{w'\rho_v'} - \rho_a\left(1 + \frac{m_a\rho_v}{m_v\rho_a}\right)\beta_{dT}\frac{\delta\overline{w'T'}}{\overline{T}} + \delta\overline{w'c'}, \quad (15)$$

where only the uncertainties in the empirical β coefficient and the covariances are considered. The covariance uncertainties are expressed as

$$\delta\overline{w'\rho_v'} = B_v + (R_{ev} + R_{tv})\overline{w'\rho_v'}, \quad (16)$$

$$\delta\overline{w'c'} = B_c + (R_{ec} + R_{tc})\overline{w'c'}, \quad (17)$$

where the $B_x$ are biases in the covariances associated with sensor errors, inadequate characterization of the cross talks, and errors in motion correction; $R_{ex}$ is similar to $B_x$ but scales proportionally to the covariance (i.e., the larger the flux, the larger the expected bias); and $R_{tx}$ characterizes the normal statistical sampling error, which decreases with the number of independent samples $N$. In this analysis, $B_c$ represents the uncertainty in the gyroscopic cross talk correction described in section 3.3.4. Combining these terms leads to a final expression for the uncertainty in the average $CO_2$ flux computed, for example, in wind speed bins

$$\delta(< F_c >) = \delta F_v + \delta F_T + \delta F_c, \quad (18)$$

$$\delta F_v = -\left[(\beta_{dv} + \beta)(R_{ev} + R_{tv}/N^{1/2}) + \delta\beta\right] \cdot < \overline{w'\rho_v'} > - (\beta_{dv} + \beta)B_v, \quad (19)$$

$$\delta F_T = -\beta_T\rho_a\left(1 + \frac{m_a\rho_v}{m_v\rho_a}\right) \cdot \left[(R_{eT} + R_{tT}/N^{1/2}) < \overline{w'T'} > + B_T\right]/\overline{T}, \quad (20)$$

$$\delta F_c = (R_{ec} + R_{tc}/N^{1/2}) < \overline{w'c'} > + B_c, \quad (21)$$

where the angle brackets indicate an ensemble average.

In the case where the signals are thermalized before detection the sensible heat flux and $\delta < F_T >$ terms are neglected. From Table 1 of *Fairall et al.* [1996] the uncertainty coefficients for water vapor flux are given by $B_v = 1.6 \times 10^{-3}$ g m$^{-2}$ s$^{-1}$, $R_{ev} = 0.05$, and $R_{tv} = 0.30$ for a 30-min sample. There are a total of 670 flux samples spread over 16 wind speed bins; for simplicity, assume that $N = 42$ for each bin. Using these values in (19) gives

$$\delta F_v = \left[\pm 7.6\times10^{-4}(\pm 0.05 \pm 0.3/42^{1/2}) \pm 1.4\times10^{-5}\right] \cdot < \overline{w'\rho_v'} > \pm\ 7.6\times10^{-4}B_v, \quad (22)$$

where the plus or minus symbol is used to indicate terms that

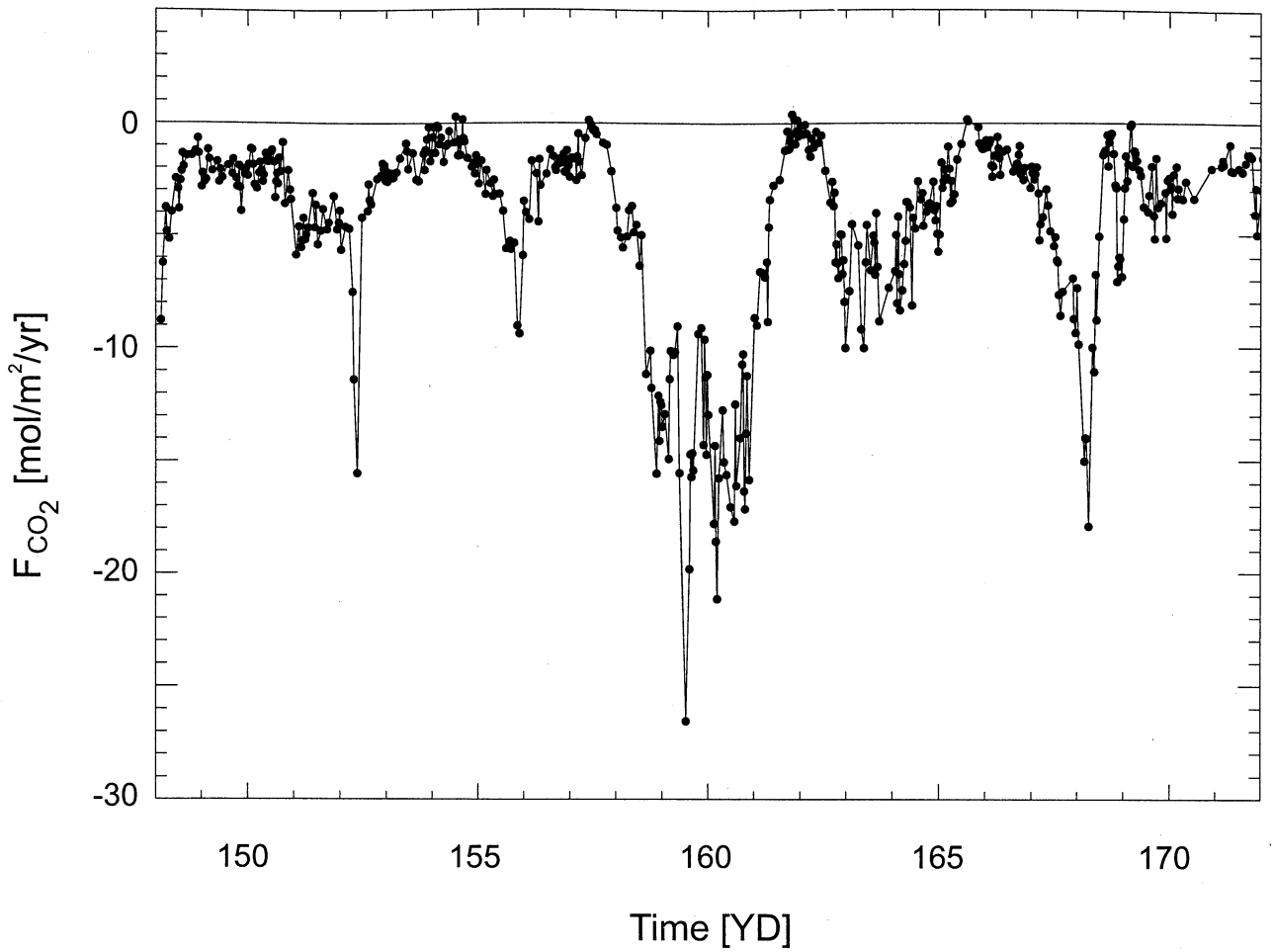


**Figure 7.** Time series of measured air-sea $CO_2$ flux.

are combined randomly (i.e., the square root of the sum of the squares). In this case, $< w'\rho_v' >$ represents the mean water vapor flux in the wind speed bin of interest. Evaluating the various terms by taking the square root of the sum of the squares yields

$$\delta F_v = \pm 5.4 \times 10^{-5} < \overline{w'\rho_v'} > \pm 1.22 \times 10^{-6}\,\mathrm{g\,m^{-2}\,s^{-1}}. \quad (23)$$

The average water vapor flux for GasEx-98 was 40 W m$^{-2}$, which is equivalent to 1.6 × 10$^{-2}$ g m$^{-2}$ s$^{-1}$. For the values selected here, this yields an uncertainty of ±1.07 mol m$^{-2}$ yr$^{-1}$. Note that if the sampling-based term $R_w/N^{1/2}$ is dropped, the bias terms yield an uncertainty of ±0.99 mol m$^{-2}$ yr$^{-1}$. Thus sampling uncertainty of water vapor dilution and cross talk makes a negligible contribution to the bias error in mean $CO_2$ flux measurements when at least 40 samples are used. Furthermore, even if the mean water vapor flux is zero, biases in its measurement will contribute a $CO_2$ flux uncertainty of ±0.87 mol m$^{-2}$ yr$^{-1}$.

For $CO_2$ the 160 calibration points $N_c$ described in section 3.3.4 imply that the slope of the linear regression of the correction with wind speed is not statistically significant (that is, the correlation coefficient of 0.11 is approximately the "no significance" value of $(N_c - 3)^{-1/2} = 0.08$). Thus the uncertainty in the gyroscopic correction is assumed to be caused by random sampling error, and the mean correction is uncertain by $B_c \approx 2.3/N_c^{1/2} = \pm 0.2$ mol m$^{-2}$ yr$^{-1}$. In this case, $B_c$ must be approximated as

$$B_c = \pm 0.2 \pm 2.3/N^{1/2}. \quad (24)$$

The flux bias that scales with the $CO_2$ flux is expected to be larger than the water vapor flux bias because of the additional uncertainties caused by tube loss and the sampling delay. This term is difficult to quantify, so a conservative value of 20% (i.e., $R_{ec} \approx 0.2$) has been chosen to represent this uncertainty. *Fairall et al.* [2000] have shown that $R_{tc}$ is 1.4 for wind speeds less than 5 m s$^{-1}$ and goes approximately as $7/U$ for wind speeds greater than 5 m s$^{-1}$. Choosing a typical value of 1.0, the error in $CO_2$ flux associated with the $CO_2$ covariance can be evaluated by

$$\begin{aligned}\delta F_c &= (\pm 0.2 \pm 1.0/42^{1/2}) < \overline{w'c'} > \\ &\pm 0.2 \pm 2.3/42^{1/2} = \pm 0.25 < \overline{w'c'} > \pm 0.41.\end{aligned} \quad (25)$$

Using this expression, the mean $CO_2$ flux at the average observed wind speed can be expressed as 4.6 ± 1.2 mol m$^{-2}$ yr$^{-1}$. A value of 20 mol m$^{-2}$ yr$^{-1}$ for one of the higher-wind-speed bins is uncertain by roughly 25%. Note that a bias in uncertainties of ~ 0.97 mol m$^{-2}$ yr$^{-1}$ will remain even if the number of samples is increased significantly. These results suggest that for the GasEx-98 experiment, water vapor cross

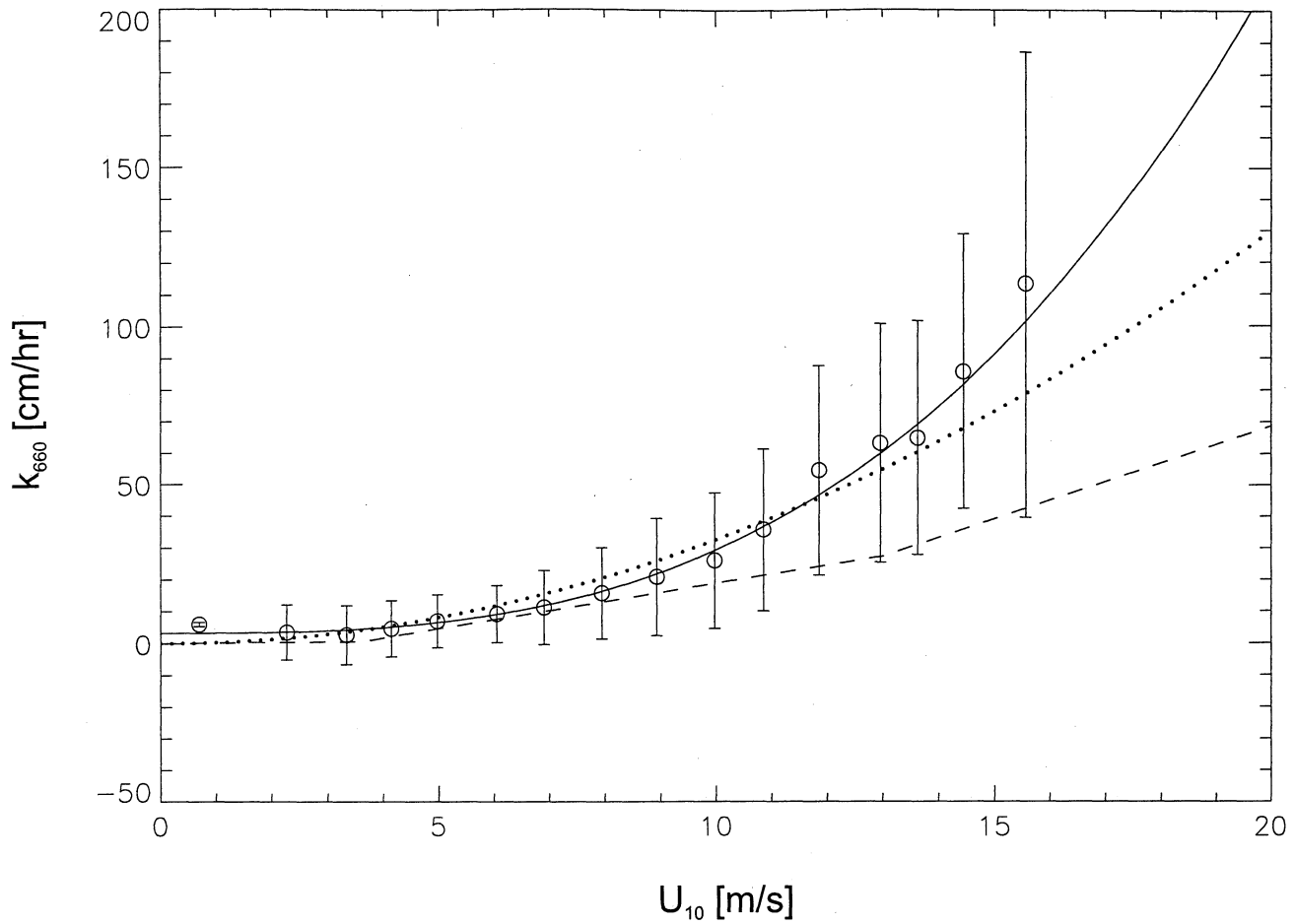


**Figure 8.** Direct covariance air-sea $CO_2$ transfer velocities and standard deviations corrected to $Sc$ = 660 versus 10-m wind speed during GasEx-98. The *Wanninkhof* [1992] relationship (dotted line), *Liss and Merlivat* [1986] relationship (dashed line), and the cubic wind speed relationship (29) (solid line).

talk and dilution uncertainties as well as $CO_2$ covariance and gyroscopic contaminations contribute equally to a typical bin-averaged flux uncertainty of $\delta(< F_c >) = \pm 1.6$ mol m$^{-2}$ yr$^{-1}$.

### 4.4. Indirect Flux Methods

**4.4.1. Bulk Formula.** The computation of fluxes using the direct covariance method is a challenging task from moving platforms. As a result, some investigations will continue to rely on indirect methods for computation of air-sea fluxes. For accurate scientific characterization of global thermal forcing, scientists must make every effort to develop indirect parameterizations of gas transfer rates based on the empirical knowledge taken from open-ocean measurements.

Of these indirect approaches the most commonly used are the bulk and bulk aerodynamic methods. As shown in (1), the flux of $CO_2$ between the atmosphere and ocean is commonly estimated using a bulk formula that relates the flux to the air-sea concentration difference via a gas transfer velocity [*Wanninkhof*, 1992]:

$$F_{CO_2} = k_{CO_2} s \Delta pCO_2 , \qquad (26)$$

where the solubility of $CO_2$ in seawater is included because the difference is expressed in terms of partial pressures as shown by (8). The transfer velocity for $CO_2$ is computed by dividing the covariance flux estimates by the air-sea $CO_2$ concentration difference. Transfer velocities are commonly normalized to a value corresponding to a nominal Schmidt number, $Sc$ = 660, through the following relationship which accounts for differences in gas diffusivity:

$$k_{660} = k\left(\frac{660}{Sc}\right)^{-1/2} , \qquad (27)$$

where $k$ is the transfer velocity for any gas.

The uncertainty analysis shows that the uncertainty is reduced in the individual estimates by bin averaging the results. However, since bin averaging does not remove any of the systematic errors/biases in the measurements, the overall biases are taken into account by reducing the measured fluxes using the linear fit to the data shown in Figure 2. Using this procedure, we bin average the normalized transfer velocity in wind speed bins. The bin-averaged values of the transfer velocity are plotted versus the 10-m wind speed in Figure 8. The standard deviations were calculated for each bin-averaged transfer velocity. The 10-m wind speed has been corrected to neutral conditions using Monin-Obukhov (MO) similarity theory [e.g., *Fairall and Markson*, 1987]. The correction, which attempts to remove the effects of atmospheric stability, is given by

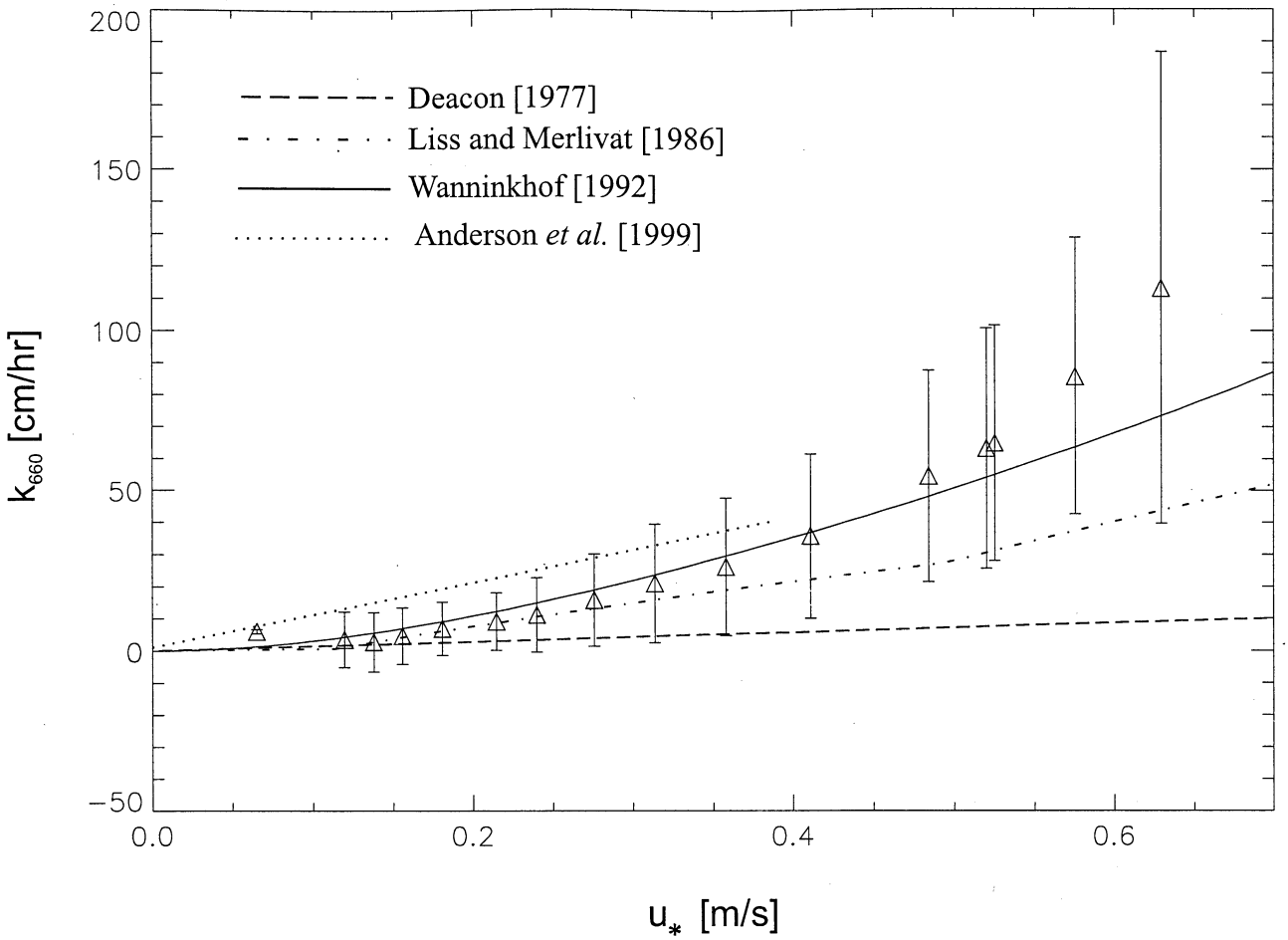


**Figure 9.** Direct covariance air-sea $CO_2$ transfer velocities and standard deviations corrected to $Sc$ = 660 versus friction velocity during GasEx-98. *Wanninkhof* [1992], *Liss and Merlivat* [1986], *Deacon* [1977], and *Anderson et al.* [1999] relationships are shown for comparison. *Anderson et al.* [1999] data are from direct flux measurements over a lake. Referenced wind speeds are converted to friction velocities using bulk drag coefficients.

$$U_N(z) = U(z) + \frac{u_*}{\kappa}\psi_m\left(\frac{z}{L}\right), \tag{28}$$

where $\kappa$ is the von Karman constant, $\psi_m$ is the stability function for momentum, and $L$ is the MO length. The function described by *Fairall et al.* [1996] is used in the analyses. The $CO_2$ transfer velocity is water-side controlled and no definitive expression for neutral conditions is established at this time.

The line fit through the measurements in Figure 8 describes a cubic dependence on wind speed given by the relationship

$$k_{660} = 3.3 + 0.026\, u_{10}^3 \tag{29}$$

where $u_{10}$ is in m s$^{-1}$ to give $k_{660}$ in cm h$^{-1}$ and the bias was removed from the fluxes before computation of the transfer velocity. The relationships of *Wanninkhof* [1992] and *Liss and Merlivat* [1986] are also shown in Figure 8 for comparison. The *Wanninkhof* [1992] gas transfer velocity has a quadratic relationship with wind speed that satisfies the global $^{14}C$ constraint, while the *Liss and Merlivat* [1986] relationship is based on laboratory and lake gas exchange experiments. In neither relationship are direct gas flux measurements considered. The cubic dependence on wind speed has also been shown by *Monahan and Spillane* [1984] and *Wanninkhof and McGillis* [1999]. *Wanninkhof and McGillis* [1999] satisfied the global isotopic constraint with a cubic dependence on wind speed, believed to be a necessary condition for air-sea gas exchange. This constraint is based on comparisons with the transfer velocities derived from bomb $^{14}C$ inventory in the ocean presented by *Broecker et al.* [1986] and was satisfied in the studies of *Wanninkhof* [1992] and *Erickson* [1993].

The main reason that both a quadratic and a cubic relationship can be shown to satisfy this constraint is that the transfer velocities computed from this inventory are limited to approximately 4.5 and 7.5 m s$^{-1}$. At the lower wind speeds, the GasEx-98 results show a finite positive transfer velocity. While some of this is attributable to the biases described above, it is interesting to note that neither the transfer nor the friction velocities tend to zero as quickly as the mean wind. Numerous studies have shown that there can be appreciable flux in extremely low wind conditions. The flux is driven by transport processes that cannot be parameterized from the mean wind speed or wind profile (i.e., the wind shear). For example, appreciable exchange of momentum, heat, and mass is possible at low winds because of large convective eddies

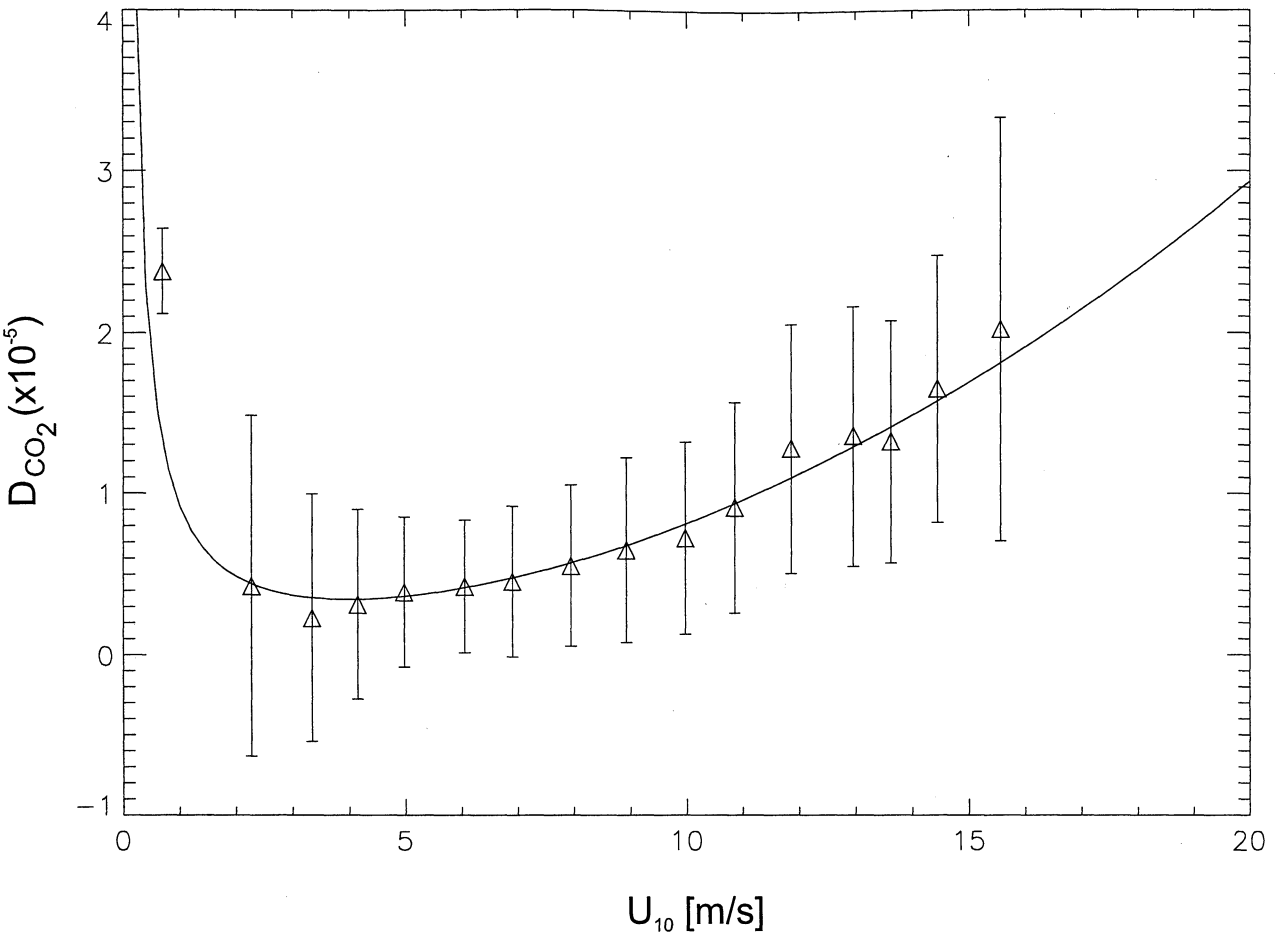


**Figure 10.** Dalton number and standard deviations for $CO_2$ transfer versus 10-m wind speed.

that span the atmospheric boundary layer. These eddies generate shear variance and turbulent transport which are difficult to parameterize.

In the Tropical Ocean-Global Atmosphere Coupled Ocean-Atmosphere Response Experiment (TOGA COARE) algorithm [*Fairall et al.*, 1996] an attempt is made to parameterize the exchange caused by these eddies through the use of a gustiness parameter. This gustiness parameter is closely related to the convective velocity scale introduced by *Deardorff* [1970] as described by *Godfrey and Beljaars* [1991]. While this flux parameterization has improved the performance of models in light wind conditions, the physical processes responsible for the transfer, particularly for gas exchange, require further study.

At wind speeds greater than 11 m s$^{-1}$ the measured transfer velocities are higher than either the *Wanninkhof* [1992] or *Liss and Merlivat* [1986] parameterizations. *Asher and Wanninkhof* [1998] and *Fairall et al.* [2000] discuss the physical processes that may contribute to the enhanced exchange, mostly owing to breaking waves and bubble mediation. Therefore some of the uncertainty in this parameterization is simply because wind speed is not the only parameter limiting the gas flux. A relationship that is commonly used to represent the physical processes controlling the aqueous mass boundary layer is given in terms of the friction velocity by

$$k = \beta^{-1} u_* Sc^{-n}; \quad (30)$$

here the variable $\beta$ is dependent on the flow Reynolds number. The exponent $n$ describes the Schmidt number dependence of the surface rheology and varies from 0.67 to 0.4. The relationship between the $CO_2$ transfer velocity and friction velocity is shown in Figure 9. The *Wanninkhof* [1992] and *Liss and Merlivat* [1986] parameterizations are plotted using $u_*$ calculated from the TOGA COARE algorithm. Recent direct measurements from a lake [*Anderson et al.*, 1999] are also shown for comparison. These results indicate that the accurate parameterization of $k$ via (30) requires further investigations of how $\beta$ depends on sea state, for example.

**4.4.2. Bulk aerodynamic formula.** Modified versions of the more common expressions used to compute the momentum, heat, and water vapor fluxes are the bulk aerodynamic formulae. For momentum the formula assumes that the drag of the atmosphere on the surface should be proportional to the wind speed squared

$$\tau = \rho_a u_*^2 = \rho_a C_D U_r^2, \quad (31)$$

where $C_D$ is a constant of proportionality known as the drag coefficient and $U_r$ is the wind speed relative to the surface. The drag coefficient can be thought of as a measure of the surface roughness. Similar expressions for the heat, water vapor, and gas fluxes can be written. The bulk aerodynamic formula for the air-sea $CO_2$ flux can be written

$$F_{CO_2} = D_{CO_2} U_r s \Delta pCO_2 \quad (32)$$

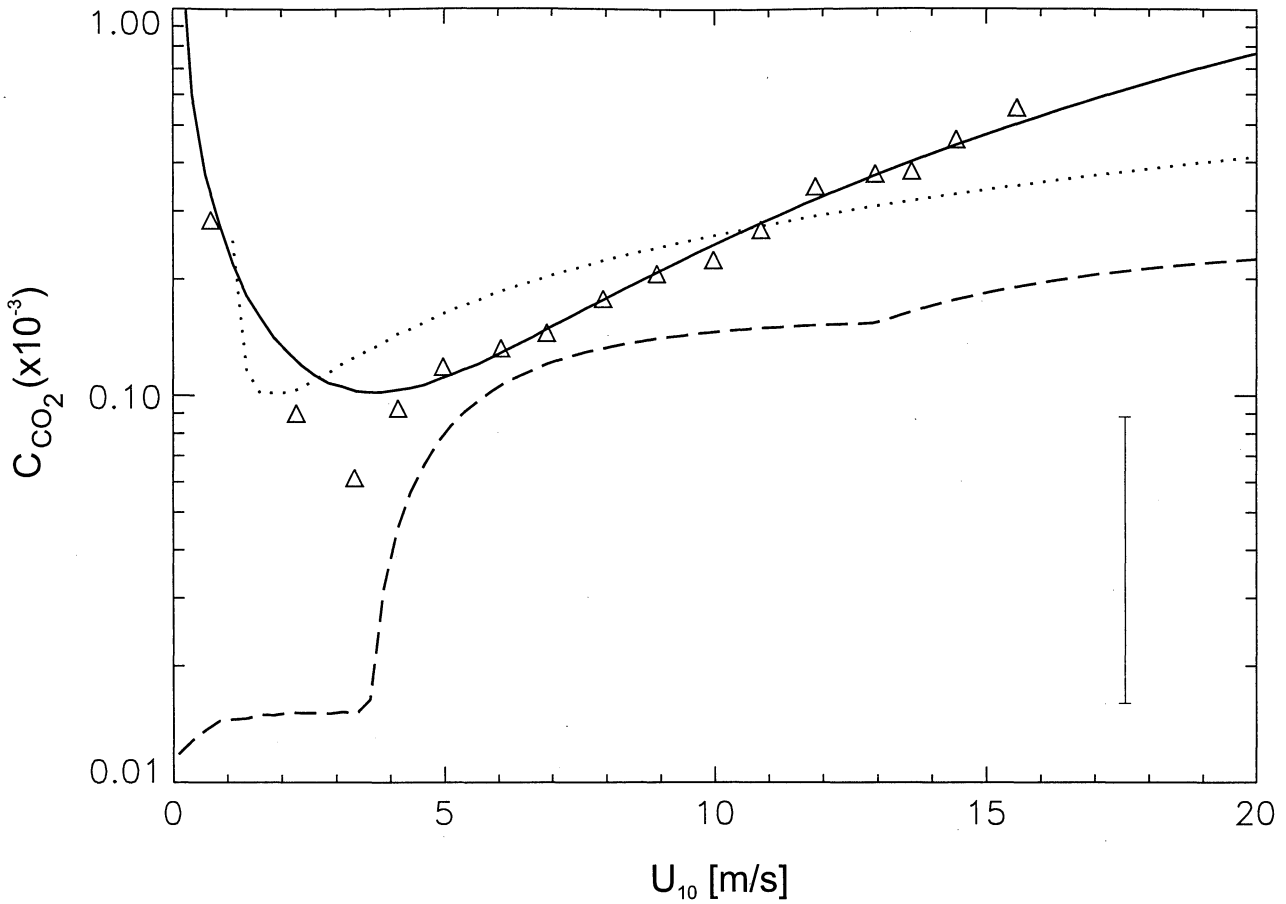


**Figure 11.** $CO_2$ transfer coefficient $C_{CO2}$ versus 10-m wind speed. The *Liss and Merlivat* [1986] results (dashed line), the *Wanninkhof* [1992] results (dotted line), and the cubic (solid line) parameterizations are shown for comparison. The average standard deviation is shown in the bottom right corner.

where $D_{CO_2}$ is the Dalton number, defined here by $k_{CO_2}/U_r$. The Dalton number plotted versus wind speed is shown in Figure 10 and is consistent with the trends from laboratory measurements [*Ocampo-Torres and Donelan*, 1994]. A minimum is observed near a 3 m s$^{-1}$ wind speed, while for winds in excess of 3 m s$^{-1}$ the Dalton number monotonically increases. This confirms that the processes controlling $CO_2$ transfer, namely, the processes of the aqueous boundary layer, are not the same as the process controlling the water vapor flux [*Ocampo-Torres and Donelan*, 1994].

Another common approach is to define the Dalton number in terms of the drag coefficient and an additional transfer coefficient

$$D_{CO_2} = C_{CO_2} C_D^{1/2}, \tag{33}$$

where $C_{CO_2}$ is the $CO_2$ transfer coefficient defined as $k_{CO_2}/u_*$. This coefficient is closely related to $\beta$ in (30). Rearranging (32), using (31) and (33), as

$$F_{CO_2} = C_{CO_2} u_* s \Delta pCO_2 \tag{34}$$

removes the need for a drag coefficient parameterization.

The separation of the Dalton number into these two components allows improvements to both the drag coefficient and gas transfer coefficients to proceed concurrently. For example, as improvements to parameterizations of $C_{CO_2}$ and $C_D$ are made, they can be easily combined to obtain improved estimates of the transfer velocity given by

$$k_{CO_2} = C_D^{1/2} U_r C_{CO_2}. \tag{35}$$

This type of parameterization of the transfer velocity would be expected to perform better in both the open ocean (generally smaller drag coefficient for a given $U_r$) and coastal sea (generally larger drag coefficient for a given $U_r$).

The $CO_2$ transfer coefficient plotted versus wind speed is shown in Figure 11. The transfer coefficient should be constant if the same processes govern air-sea $CO_2$ exchange and momentum exchange. The hypothesis is that the enhancement of the transfer coefficient is more a result of bubble mediation than wave breaking. This hypothesis is based on the assumption that the enhancement of the transfer velocity due to wave breaking is removed after normalization by the friction velocity; that is, this enhancement is mainly due to enhanced drag. The enhancement of the gas exchange due to bubble mediation is not expected to be removed by this normalization. Unfortunately, these two effects are difficult to study separately in the field.

Field estimates can be compared to laboratory results of *Frew et al.* [1995] by plotting the transfer coefficient versus the roughness Reynolds number as shown in Figure 12. The roughness Reynolds number is defined as

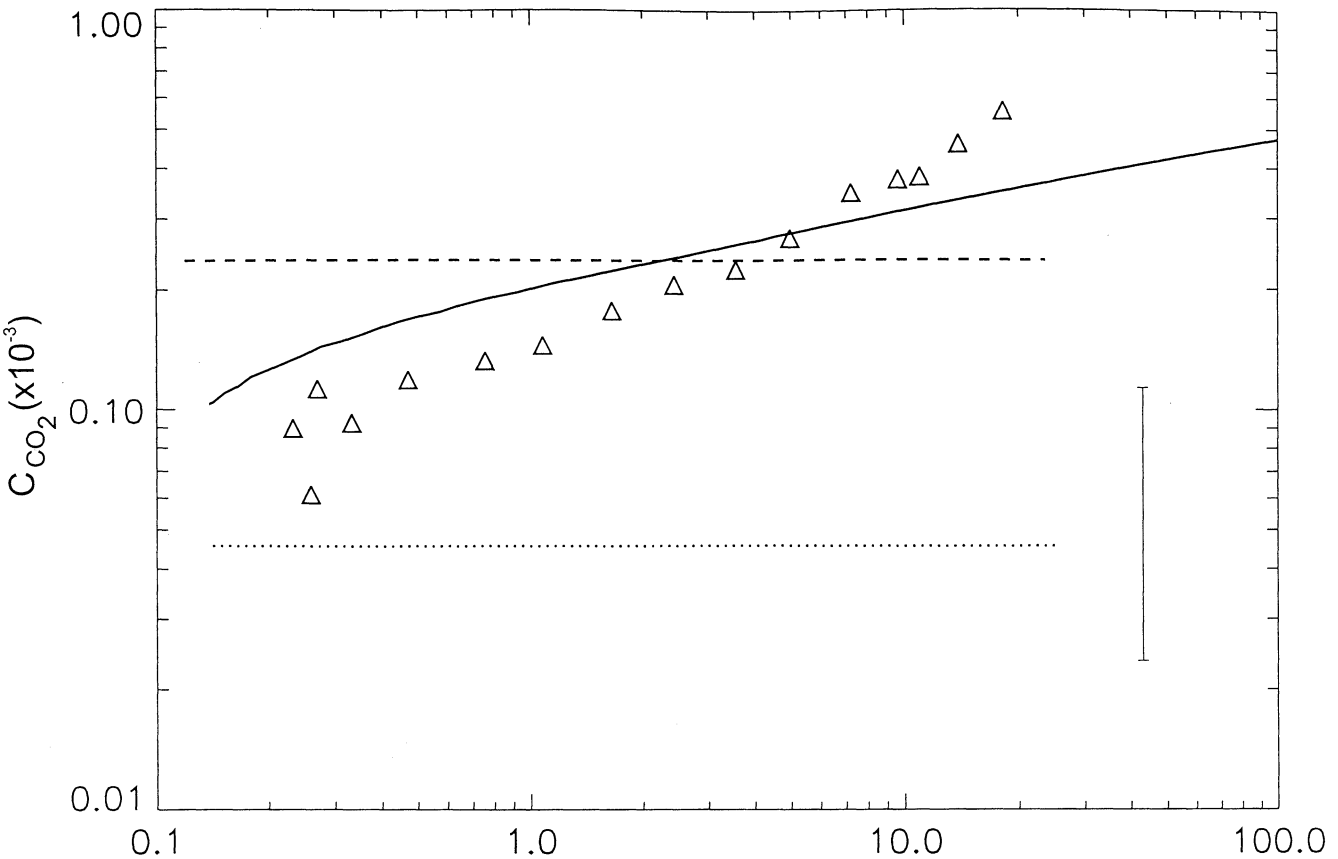


**Figure 12.** $CO_2$ transfer coefficient $C_{CO2}$ versus roughness Reynolds number $Re_*$. The *Wanninkhof* [1992] results (solid line), laboratory clean results (dashed line), and laboratory results with surfactants (dotted line) are shown for comparison. The average standard deviation is shown in the bottom right corner.

$$Re_* = \frac{z_0 u_*}{\nu_a}, \tag{36}$$

where $z_0$ is the velocity roughness height. The transfer coefficient for $CO_2$ measured during GasEx-98 continuously increases with $Re_*$. Shown for comparison are the laboratory results for a clean surface, laboratory results with surface films, and the *Wanninkhof* [1992] relationship. At small $Re_*$ the field data are between the clean and surface film results. At higher $Re_*$ both the Wanninkhof relationship and the field data increase above the laboratory results. This is attributed to the fact that the laboratory measurements do not provide the scales of the ocean environment. At even greater $Re_*$ the field data increase faster than those of Wanninkhof, which is consistent with the results shown in Figure 11.

## 5. Conclusions

Direct covariance air-sea $CO_2$ flux measurements were performed over the open ocean during GasEx-98. The environmental conditions in the North Atlantic were optimal for accurate direct covariance $CO_2$ flux measurements. A relatively large $pCO_2$ air-sea difference was maintained within the study area with relatively low $H_2O$ fluxes. The high $CO_2$ fluxes and low $H_2O$ fluxes increased the SNR for increased measurement accuracy. Some uncertainties in $CO_2$ flux measurements were caused by ship motion. The half-hour mean wind speeds varied over a wide range from 0.9 to 16.3 m $s^{-1}$ resulting in an average $CO_2$ flux of 4.6 mol $m^{-2}$ $yr^{-1}$ into the ocean.

For the first time, covariance measurements of $CO_2$ transfer velocity are in general agreement with the isotopic and indirect methods results. In particular, there is good agreement for wind speeds less than 11 m $s^{-1}$. The measurements for higher wind speeds show a general enhancement of gas transfer velocity over the indirect methods. This enhancement may be explained by the fact that the indirect methods cannot discriminate surface process variability such as atmospheric stability, upper-ocean mixing, wave age, wave breaking, or surface films. To understand the relationship between gas physical properties, surface processes, and air-sea $CO_2$ exchange, direct $CO_2$ flux measurements are crucial.

**Acknowledgments.** This work was supported by the National Science Foundation Grant OCE-9711218 and NOAA Global Carbon Cycle in the Office of Global Programs. The authors wish to thank the crew of the NOAA R/V *Ronald H. Brown* for their outstanding

efforts. Thanks are also given to the anonymous reviewers for their helpful comments and suggestions. This is Woods Hole Oceanographic Institution contribution 10352.

## References


Anderson, D. E., R. G. Striegl, D. I. Stannard, C. M. Michmerhuizen, T. A., McConnaughey, J. W. LaBaugh, Estimating lake-atmosphere $CO_2$ exchange, *Limnol. Oceanogr.*, 44(4), 988-1001, 1999.

Asher, W. E., and R. Wanninkhof, The effect of bubble-mediated gas transfer on purposeful dual gaseous-tracer experiments, *J. Geophys. Res., 103*, 10,555-10,560, 1998.

Broecker, H. C., J. Petermann, and W. Siems, The influence of wind on $CO_2$-exchange in a wind/wave tunnel including the effects of monolayers, *J. Mar. Res., 36*, 595-610, 1978.

Broecker, W. S., and T.-H. Peng, *Tracers in the Sea*, Lamont-Doherty Earth Observatory, Palisades, N.Y., 1982.

Broecker, W. S., J. R. Ledwell, T. Takahashi, R. Weiss, L. Merlivat, L. Memery, T. H. Peng, B. Jähne, and K. O. Munnich, Isotopic versus micrometeorologic ocean $CO_2$ fluxes: A serious conflict, *J. Geophys. Res., 91*, 10,517-10,527, 1986.

Businger, J. A., On the measurement of the transfer of gases across the air-sea interface, *J. Appl. Meteorol., 36*, 1113-1115, 1997.

Deacon, E. L., Gas transfer to and across an air-water interface. *Tellus*, 29, 363-374, 1977.

Deardorff, J. W., Convective velocity and temperature scales for the unstable planetary boundary layer and for Rayleigh convection, *J. Atmos. Sci., 27*, 1211-1213, 1970.

Edson, J. B., A. A. Hinton, K. E. Prada, J. E. Hare, and C. W. Fairall, Direct covariance flux estimates from mobile platforms at sea, *J. Atmos. Oceanic Technol., 15*, 547-562, 1998.

Erickson, D. J., III, A stability-dependent theory for air-sea gas exchange, *J. Geophys. Res., 98*, 8471-8488, 1993.

Fairall, C. W., and R. Markson, Mesoscale variations in surface stress, heat fluxes, and drag coefficient in the Marginal Ice Zone Experiment, *J. Geophys. Res., 92*, 6921-6932, 1987.

Fairall, C. W., E. F. Bradley, D. P. Rogers, J. B. Edson, and G. S. Young, Bulk parameterization of air-sea fluxes for TOGA COARE, *J. Geophys. Res., 101*, 3747-3764, 1996.

Fairall, C. W., J. E. Hare, J. B. Edson, and W. R. McGillis, Measurement and parameterization of air-sea gas transfer, *Boundary Layer Meteorol., 96*, 63-105, 2000.

Frew, N. M., E. J. Bock, W. R. McGillis, A. Karachintsev, and T. Hara, Parameterization of air-water gas transfer using wind stress and viscoelasticity, in *Air-Water Gas Transfer,* edited by B. Jähne and E. Monahan, pp. 529-541, AEON Verlag, Hanau, Germany, 1995.

Godfrey, J. S., and A. C. M. Beljaars, On the turbulent fluxes of buoyancy, heat, and moisture at the air-sea interface at low wind speeds, *J. Geophys. Res., 96*, 22,043-22,048, 1991.

Jähne, B., On transfer processes at a free air-water interface, Habilitation thesis, Fac. of Phys. and Astron., Univ. of Heidelberg, Heidelberg, Germany, 1985.

Jähne, B., and E. C. Monahan (Eds.), *Air-Water Gas Transfer*, 899 pp., AEON Verlag, Hanau, Germany, 1995.

Jähne, B., K. O. Münnich, R. Bösinger, A. Dutzi, W. Huber, and P. Libner, On the parameters influencing air-water gas exchange, *J. Geophys. Res., 92*, 1937-1949, 1987.

Jones, E. P., and S. D. Smith, A first measurement of sea-air $CO_2$ flux by eddy correlation, *J. Geophys. Res., 82*, 5990-5992, 1977.

Kaimal, J. C., J. C. Wyngaard, Y. Izumi, and O. R. Cote, Spectral characteristics of surface-layer turbulence, Q. J. R. Meteorol. Soc., *98*, 563-589, 1972.

Kohsiek, W., Water vapor cross-sensitivity of open path $H_2O/CO_2$ sensors, *J. Atmos. Oceanic Technol., 17*, 299-311, 2000.

Lenschow, D. H., and M. R. Raupach, The attenuation of fluctuations in scalar concentrations through sampling tubes, *J. Geophys. Res., 96*, 5259-5268, 1991.

Leuning, R., and M. J. Judd, The relative merits of open- and closed-path analyzers for measurement of eddy fluxes, *Global Change Biol., 2*, 241-253, 1996.

Leuning, R., and J. Moncrieff, Eddy covariance $CO_2$ flux measurements using open- and closed-path $CO_2$ analysers: Corrections for analyser water vapour sensitivity and damping of fluctuations in air sampling tubes, *Boundary Layer Meteorol., 53*, 63-76, 1990.

Liss, P. S., and L. Merlivat, Air-sea gas exchange rates: Introduction and synthesis, in *The Role of Air-Sea Exchange in Geochemical Cycling,* edited by P. Buat-Ménard, pp. 113-129, D. Reidel, Norwell, Mass., 1986.

Liss, P. S., and P. G. Slater, Flux of gases across the air-sea interface, *Nature, 247*, 181-184, 1974.

Mahrt, L., D. Vickers, J. Howell, J. Højstrup, M. Courtney, J. M. Wilczak, J. Edson, and J. Hare, Sea surface drag coefficients in the Risø Air Sea Experiment, *J. Geophys. Res., 101*, 14,327-14,335, 1996.

Massman, W. J., The attenuation of concentration fluctuations in turbulent flow through a tube, *J. Geophys. Res., 96*, 5269-5273, 1991.

McGillis, W. R., J. W. H. Dacey, N. M. Frew, E. J. Bock, and B. K. Nelson, Water-air flux of dimethylsulfide, *J. Geophys. Res., 105*, 1187-1193, 2000.

Monahan, E. C., and M. C. Spillane, The role of oceanic whitecaps in air-sea gas exchange, in *Gas Transfer at Water Surfaces*, edited by W. Brutsaert and G. H. Jirka, pp. 495-503, D. Reidel, Norwell, Mass., 1984.

Ocampo-Torres, F. J., and M. A. Donelan, Laboratory measurements of mass transfer of carbon dioxide and water vapour for smooth and rough flow conditions, *Tellus, Ser. B, 46*, 16-32, 1994.

Peng, T.-H., W. S. Broecker, G. G. Mathieu, Y. H. Li, and A. E. Bainbridge, Radon evasion rates in the Atlantic and Pacific oceans as determined during the GEOSECS program, *J. Geophys. Res., 84*, 2471-2486, 1979.

Smith, S. D., and E. P. Jones, Evidence for wind-pumping of air-sea exchange based on direct measurements of $CO_2$ fluxes, *J. Geophys. Res., 90*, 869-875, 1985.

Suyker, A. E. and S. B. Verma, Eddy correlation measurement of $CO_2$ flux using a closed-path sensor: Theory and field tests against an open-path sensor, *Boundary Layer Meteorol., 64*, 391-407, 1993.

Wanninkhof, R., Relationship between gas exchange and wind speed over the ocean, *J. Geophys. Res., 97*, 7373-7381, 1992.

Wanninkhof, R., and W. R. McGillis, A cubic relationship between air-sea $CO_2$ exchange and wind speed, *Geophys. Res. Lett., 26*, 1889-1892, 1999.

Webb, E. K., G. I. Pearman, and R. Leuning, Correction of flux measurements for density effects due to heat and water vapor transport, *Q. J. R. Meteorol. Soc., 106*, 85-100, 1980.

Wesely, M. L., D. R. Cook, R. L. Hart, and R. M. Williams, Air-sea exchange of $CO_2$ and evidence for enhanced upward fluxes, *J. Geophys. Res., 87*, 8827-8832, 1982.


J. B. Edson and W. R. McGillis, Department of Applied Ocean Physics and Engineering, Woods Hole Oceanographic Institution, MS 11, Woods Hole, MA 02543-1053. (jedson@whoi.edu; wmcgillis@whoi.edu.)

C. W. Fairall and J. E. Hare, NOAA Environmental Technology Laboratory, 325 Broadway, Boulder, CO 80303. (chris.fairall@noaa.gov; jeff.hare@noaa.gov.)

(Received June 22, 2000; revised January 17, 2001; accepted January 29, 2001.)